EFFECT OF LOW ENERGY AND HIGH CHARGE STATE OXYGEN AND NITROGEN ION BEAM IRRADIATION ON POLYMETHYL METHACRYLATE

A DISSERTATION

*Submitted in partial fulfillment of the
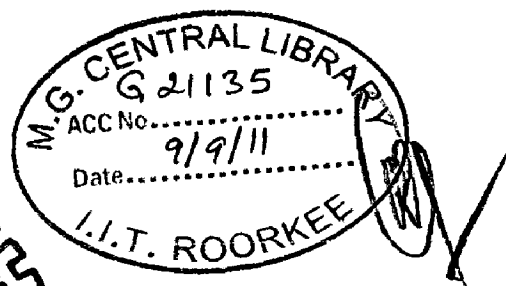requirements for the award of the degree
of*

MASTER OF TECHNOLOGY

in

NANOTECHNOLOGY

By

UMESH CHANDRA BIND

CENTRE OF NANOTECHNOLOGY
INDIAN INSTITUTE OF TECHNOLOGY ROORKEE
ROORKEE - 247 667 (INDIA)
JUNE, 2011

CANDIDATE'S DECLARATION

I hereby declare that the work which has been presented in this dissertation entitled as **"EFFECT OF LOW ENERGY AND HIGH CHARGE STATE OXYGEN AND NITROGEN ION BEAM IRRADIATION ON POLYMETHYL METHACRYLATE"** in partial fulfillment of the requirement for the award of the degree of **MASTER OF TECHNOLOGY** with specialization in **"NANOTECHNOLOGY"**, submitted in the Centre of Nanotechnology, Indian Institute of Technology, Roorkee, is an authentic record of my own work carried out by me during the period from August 2010 to June 2011 under the supervision and guidance of Dr. R. K. Dutta, Depaetment of Chemistry & Centre of Nanotechnology, Indian Institute of Technology, Roorkee.

The matter embodied in this dissertation has not been submitted by me anywhere else for the award of any other degree elsewhere.

Date: 30/6/11

Place: Roorkee

(Umesh Chandra Bind)

CERTIFICATE

This is to certify that the above statement made by the candidate **Umesh Chandra Bind** is correct to the best of my knowledge and belief.

Date: 30|6|11

Place: Roorkee

(Dr. R. K. Dutta)

Assistant professor,

Department of Chemistry &

Centre of Nanotechnology,

Indian Institute of Technology,

Roorkee-247 667

i

ABSTRACT

Surface modification of polymethyl methacrylate (PMMA) was done by using low energy and high charge state of Oxygen and Nitrogen ion implantation/irradiation facility using ECR ion source available at VECC Kolkata. Firstly, Oxygen ion beam of 7+ and 2+ charge states of energy 63 keV and doses 1×10^{16} and 1.4×10^{17} respectively were implanted on 10×10 mm^2 of 1 mm thick sheet of PMMA. Secondly, high charge state (5+) of Oxygen and Nitrogen ion beam of 45 keV energy was implanted on the 10×10 mm^2 of PMMA. The particle dose was varied between 10^{14} to 10^{17} ions/cm^2. Optical responses, (absorbance, reflectance and transmittance), dielectric responses (dielectric response, dielectric loss) and morphological studies by FE-SEM were employed to investigate structure and properties of the as-implanted PMMA samples. The dielectric constant of implanted PMMA as a function of applied frequency of electric field was found to be independent of high charge state ion, but it depends on the implanted dose. The dielectric loss of these samples varied in different frequency range for different high charge state ions. The absorbance of O^{7+} and O^{2+} implanted PMMA samples was higher in UV-Vis range and show charge state dependency. The absorbance of O^{5+} implanted PMMA samples was higher as compared to the N^{5+} implanted PMMA. Further optical absorbance for N^{5+} and O^{5+} implanted PMMA were high for high dose. The diffuse reflectivity (DR) of O^{5+} implanted PMMA samples were about two times higher than N^{5+} implanted PMMA. The DR of O^{5+} and N^{5+} implanted PMMA was found to be dose dependent. The surface morphology of O^{2+} and O^{7+} implanted PMMA samples had shrunken and ripples of different wavelength on the surface were formed. However, such ripples were not observed in the PMMA sample implanted with 45 keV O and N beams of 5+ charge state.

ACKNOWLEDGEMENT

LIST OF ABBREVIATIONS

PMMA = Poly(methyl methacrylate)

PVC = Polyvinyl chloride

PC = Polycarbonate

PTFE = Polytetrafluoroethylene

PE = Polyethylene

PP = Polypropylene

PS = Polystyrene

SHI = Swift Heavy Ion

AFM = Atomic Force Microscope

SEM = Scanning Electron Microscope

HCI = Highly Charged Ion

GCIB = Gas Cluster Ion Beam

ECR = Electron Cyclotron Resonance

UV-Vis-NIR = Ultraviolet Visible Near Infra Red

FE-SEM = Field Emission Scanning Electron Microscopy

FES = Field Emission Source

EDXA = Energy Dispersive X-ray Analysis

SRIM = Stopping and Range of Ions in Matter

DR = Diffuse Reflectivity

CONTENTS

TABLE OF CONTENTS

1 INTRODUCTION

2 LITERATURE REVIEW

3 EXPERIMENTAL & CHARACTERIZATION TECHNIQUE

4 EFFECT OF 2+ & 7+ CHARGE STATE OXYGEN ION BEAM

IMPLANTATION ON PMMA (POLYMETHYL METHACRYLATE

5 EFFECT OF N^{5+} AND O^{5+} ION BEAM IMPLANTATION ON PMMA

(POLYMETHYL METHACRYLATE)

LIST OF FIGURES

LIST OF TABLES

LIST OF PUBLICATIONS

1. Paper present "Effect of O-Ion Implantation in PMMA" in "National Workshop on Science with ECR based keV Ion Beams" held at VECC Kolkata, India, during January 20-21, 2011.

2. Paper present "Preliminary Results on the Effects of 63 keV High Charge State Oxygen Ion Beam Implantation on PMMA" in Nuclear and Radiochemistry Symposium (NUCAR 2011) held at GITAM University, Visakhapatnam, India, during February 22 - 26, 2011.

CHAPTER 1

1.1 Introduction

The surface modification is an interesting branch of research due to its various applications in science and technology. Therefore it must be done in such a way that the modification restricting to the outer few atomic layers of a material (in nanometer range) so that only a minute fraction of the material is altered such type of modification can be done low energy and high charge state ion beam irradiation [1]. This could be better than other surface modification methods, namely; chemical treatment [2, 3], plasma discharge method [4-6], laser radiation [7-11], and electron beam irradiation [12] due to its precise control of modification. The modification must be done in such a way so that the modified surface region must be stable in its application environment [13]. Since, due to few nanometer modifications, the degradation or loss of modified material can results in significant changes in its characteristics properties. Thus, the modified material (created either by deposition of new material or ion beam irradiation of the existing material) must be resistant to processes such as abrasion, chemical attack, and surface rearrangement. The degree of stability depends on the properties of the environment in which the surface-modified material is placed.

1.2 Polymeric materials

Polymer means a particular class of macromolecules, having a set of regularity repeated chemical units of the identical type, or possibly of a very limited number of different types, joined end to end or sometimes in more complex manner, to form a chain molecule. Polymers consist of many random molecular chains, with no particular orientation, and no chemical bonds existing between chains. When heat is applied to such a material, the chains are free to slip and flow under relatively small outside force. Such a material is called a thermoplastic e.g. PMMA.

1.2.1 Molecular structure

Polymers (or macromolecules) are very large molecules made up of smaller units, called monomers or repeating units, covalently bonded together (Fig. 1.1). This specific molecular structure (chainlike structure) of polymeric materials is responsible for their intriguing mechanical properties. Polymer architecture can vary. Three possible molecule architectures are depicted.
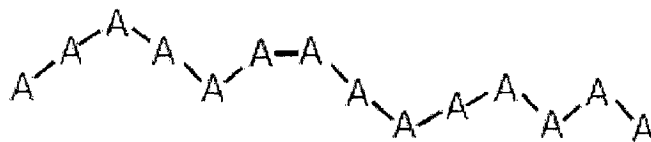
Fig. 1.1 A is a Monomer, -represents a covalent bond

A linear polymer consists of a long chain of monomers. A branched polymer has branches covalently attached to the main chain. Cross-linked polymers have monomers of one chain covalently bonded with monomers of another chain. Cross linking results in a three-dimensional

2

network; the whole polymer is a giant macromolecule. Elastomers are loosely cross-linked networks while thermosets are densely cross-linked networks.
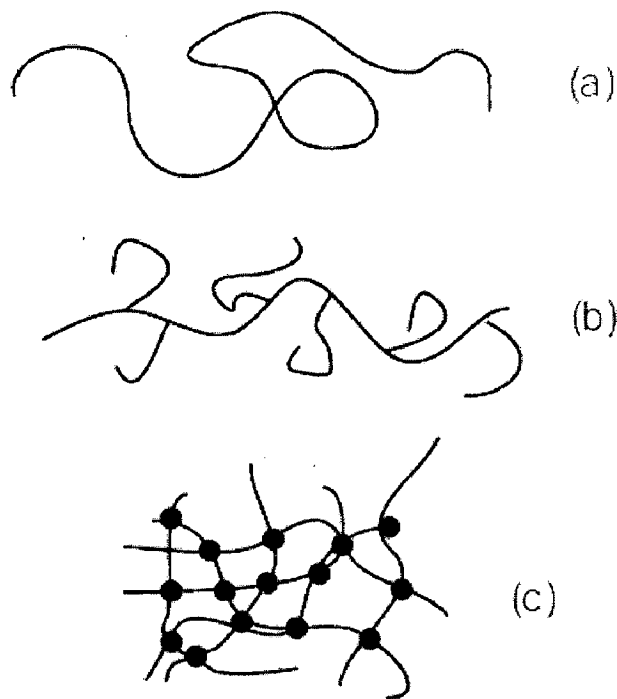
Fig. 1.2 Types of molecular configuration: (a) Linear chain. (b) Branched molecule. (c) Cross-linked network: molecules are linked through covalent bonds; the network extends over the whole sample which is a giant macromolecule.

Another classification of polymers is based on the chemical type of the monomers (Fig. 1.3) Homopolymers consist of monomers of the same type; copolymers have different repeating units. Furthermore, depending on the arrangement of the types of monomers in the polymer chain, we have the following classification:

- In random copolymers two or more different repeating units are distributed randomly

- Alternating copolymers are made of alternating sequences of the different monomers

3

- In block copolymers long sequences of a monomer are followed by long sequences of another monomer

- Graft copolymers consist of a chain made from one type of monomers with branches of another type.

-A-A-A-A-A-A-A-A-A-A-A-A-A-A-A-A-A-A-A-A-A-A-A-A-A-A-A-   (a)

-A-A-B-A-B-B-A-B-A-A-B-A-A-A-B-A-B-B-A-B-B-B-A-A-B-A-A-   (b)

-A-B-A-B-A-B-A-B-A-B-A-B-A-B-A-B-A-B-A-B-A-B-A-B-A-   (c)

-A-A-A-A-A-A-A-A-A-B-B-B-B-B-B-B-B-B-B-B-A-A-A-A-A-A-A-   (d)

```
        |
        B
        |
        B
        |
        B
        |
-A-A-A-A-A-A-A-A-A-A-A-A- A-A-A-A-A-A-A-A-A-A-A-A-A-A-A-    (e)
        |                   |
        B                   B
        |                   |
        B                   B
        |                   |
        B                   B
        |                   |
        B                   B
        |                   |
        B
        |
        B
        |
```
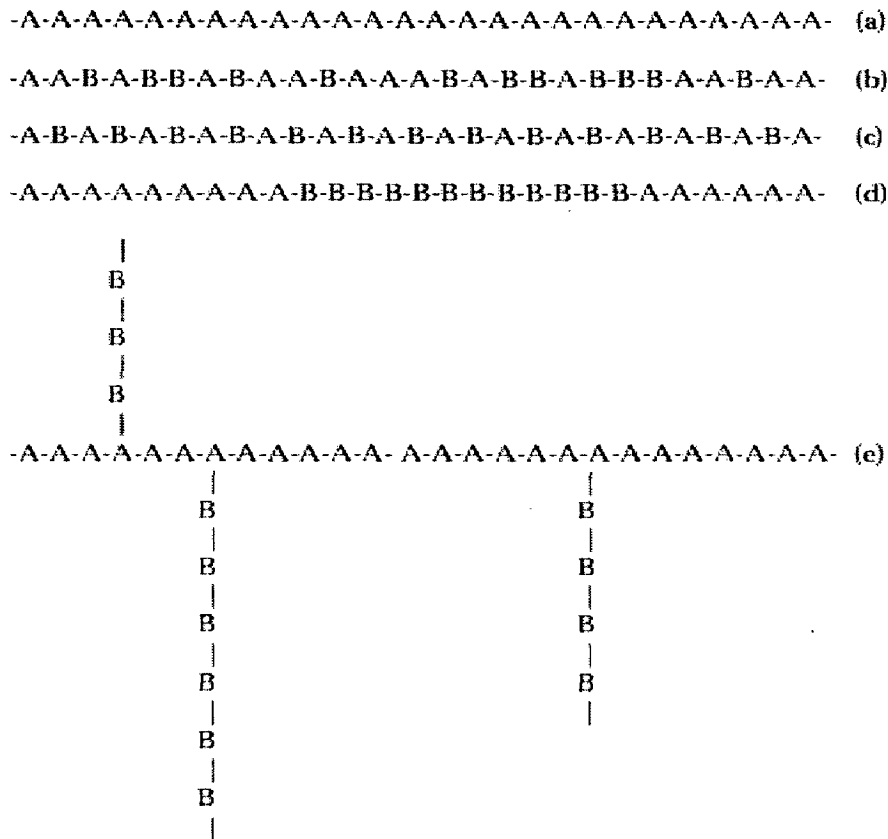
Fig. 1.3 (a) Homopolymer (b) Random copolymer (c) Alternating copolymer (d) Block copolymer (e) Graft copolymer

.2.2 Microstructure

Many properties of polymeric materials depend on the microscopic arrangement of their molecules. Polymers can have an amorphous or semi-crystalline structure (Fig. 1. 4). Amorphous polymers lack order and are arranged in a random manner, while semi-crystalline polymers are partially organized in orderly crystalline structures.
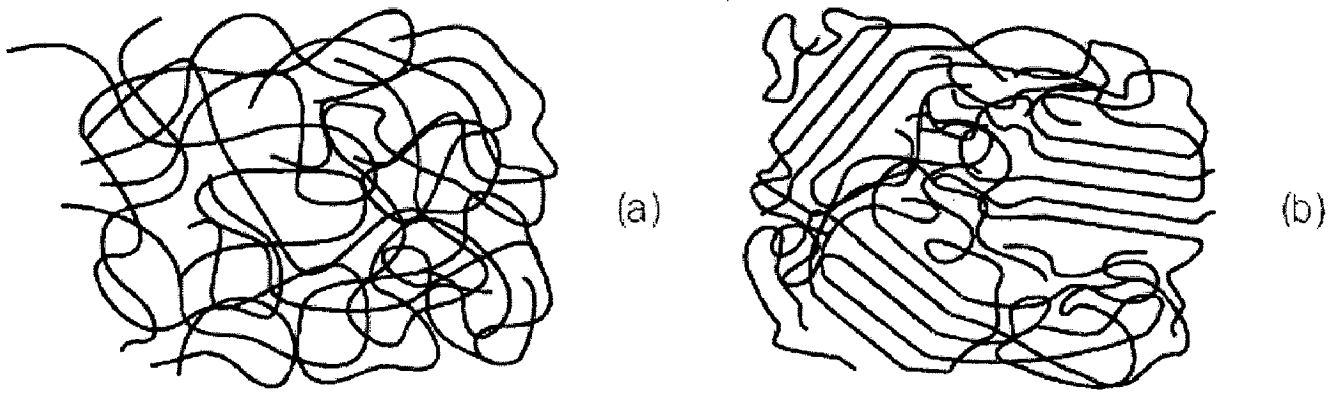
Fig. 1.4 (a) Amorphous polymer (observe the entanglements among the polymer chains) and (b) semicrystalline polymer.

1.2.3 Thermal behavior

Thermosets, which are densely cross-linked in the form of a network, degrade upon heating, while thermoplastics, which do not contain cross-links, melt upon heating.
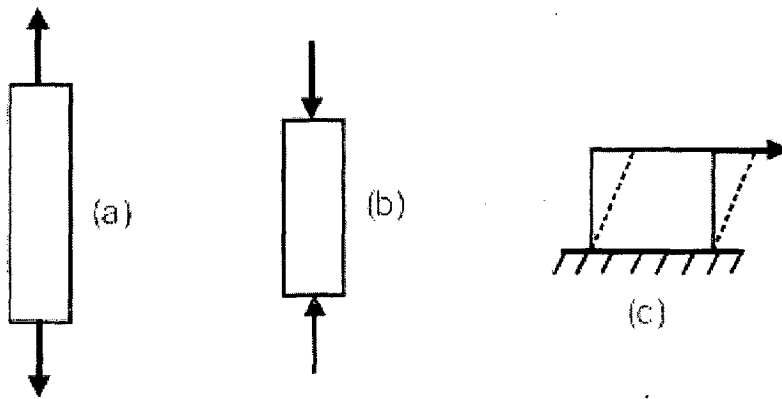
Fig. 1.5 Examples of types of forces used in slip the polymer layers: (a) tensile force. (b) Compressive force. (c) Shear force.

5

1.2.4 Composite materials

Composite materials can be developed by mixing two or more basic constituents with improved physical properties are new field of material with dramatically increasing interest. In polyme composite, the second component with very different properties is added to the polymer so that both components contribute to the properties of product. The second component often increase the properties of product, such as hardness, absorbance, reflectance, etc. Although composites are very important class of polymeric materials and they form separate class of material. It shows properties of both-Polymer matrix and added material.

1.2.5 Types of polymers on the basis of polarization

There are two types of polymers:

1- Polar

2- Non-polar

The structure of polymer determines whether it is polar or non-polar which determine dielectric properties of polymeric materials. In polar polymer materials, dipoles are created by imbalance in electric distribution and in presence of external electric field these dipole align with the field. This creates a 'dipole polarization' of polymer and due to movement of the dipoles is involved, there is time associated with the movement of dipoles. The polar polymers are PMMA, PVC, Nylon, PC, etc used as insulators.

The non-polymer materials having purely covalent and symmetrical molecules have no any polar dipole. On the application of external electric field, the electron moves slightly in its direction to create an 'electron polarization', in this case the movement is caused due to only the electron and this is effectively instantaneous. Some examples of such polymers are PTFE, PE, PP and PS which have high resistivity and low dielectric constant.

6

1.2.6 Polymethyl methacrylate (PMMA)

PMMA, a transparent thermoplastic is often preferred because of its moderate properties, easy handling and processing, and low cost, but behaves in a brittle manner when loaded, especially under an impact force, and is more prone to scratching compared to conventional inorganic glass. All commercial PMMA is atactic and completely amorphous (Fig. 1.4.a).

PMMA is a strong and lightweight material. It has a density of 1.17–1.20 g/cm^3, which is less than half that of glass. It also has good impact strength, higher than both glass and polystyrene; however, PMMA's impact strength is still significantly lower than polycarbonate and some engineered polymers.

(a)   (b)   (c)
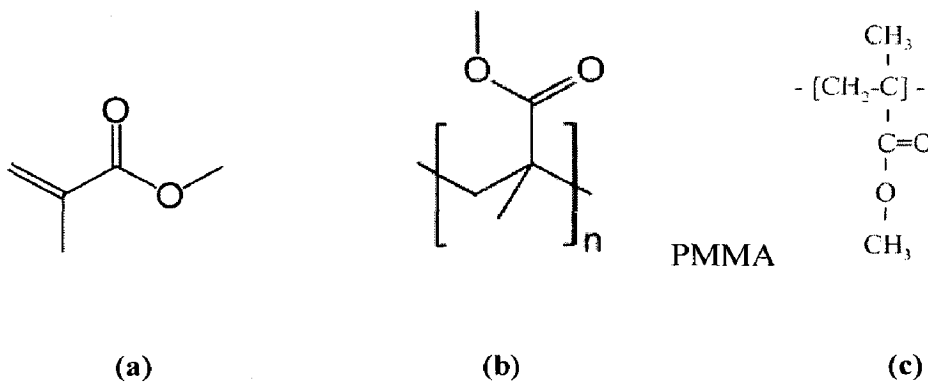
Fig. 1.6 Shechamatic diagram of (a) Monomer (b) Methyl methacrylate (c) Chemical structure of PMMA

The glass transition temperature (T_g) of atactic PMMA is 105°C. The T_g of commercial grades of PMMA range from 85 to 165 °C, the range is so wide because of the vast number of commercial compositions which are copolymers with co-monomers other than methyl methacrylate. PMMA is thus an organic glass at room temperature i.e. it is below its T_g. The forming temperature starts at the glass transition temperature and goes up from there [14].

7

As observed that PMMA of 3 mm thickness transmits up to 92% of visible light, and gives a reflection of about 4% from each of its surfaces and had refractive index 1.492 and dielectric constant 2.6 at 1MHz. It filters ultraviolet light similar to ordinary window glass. Some manufacturers add coatings to PMMA to improve absorption in the 300–400 nm range. PMMA passes infrared light of up to 2800 nm and blocks IR of longer wavelengths up to 25000 nm. Various types of colored PMMA allow to passing specific IR wavelengths while blocking visible light which could be used for heat sensor, irradiation sensor or remote control.

PMMA swells and dissolves in many organic solvents. It has also poor resistance to many other chemicals. Nevertheless, its environmental stability is superior to most other plastics such as polystyrene and polyethylene. Therefore, PMMA is the material of choice for outdoor applications. Its coefficient of thermal expansion is relatively high as $(5–10) \times 10^{-5}$ /K.

1.3 Surface modification of polymer

Surface modification of polymer is receiving increasing interest due to its widespread applications in various fields of science and technology. A number of techniques could be employed to modify polymer surface. Some of them are:

1- Chemical treatment

2- DC glow/plasma treatment

3- Laser irradiation

4- Electron beam irradiation

5- Ion beam irradiation

1.3.1 Chemical treatment

Chemical modification of organic, metallic and oxide materials surface include the reaction of surface functional groups (hydroxyl, acid, etc.), self-assembly of molecules onto surfaces, gas-phase treatments (oxidation, reduction, sulfidation, etc.), and liquid-phase treatments (e.g., acid etching)[2, 3]. Schematics of these processes are shown in Fig. 1.7.
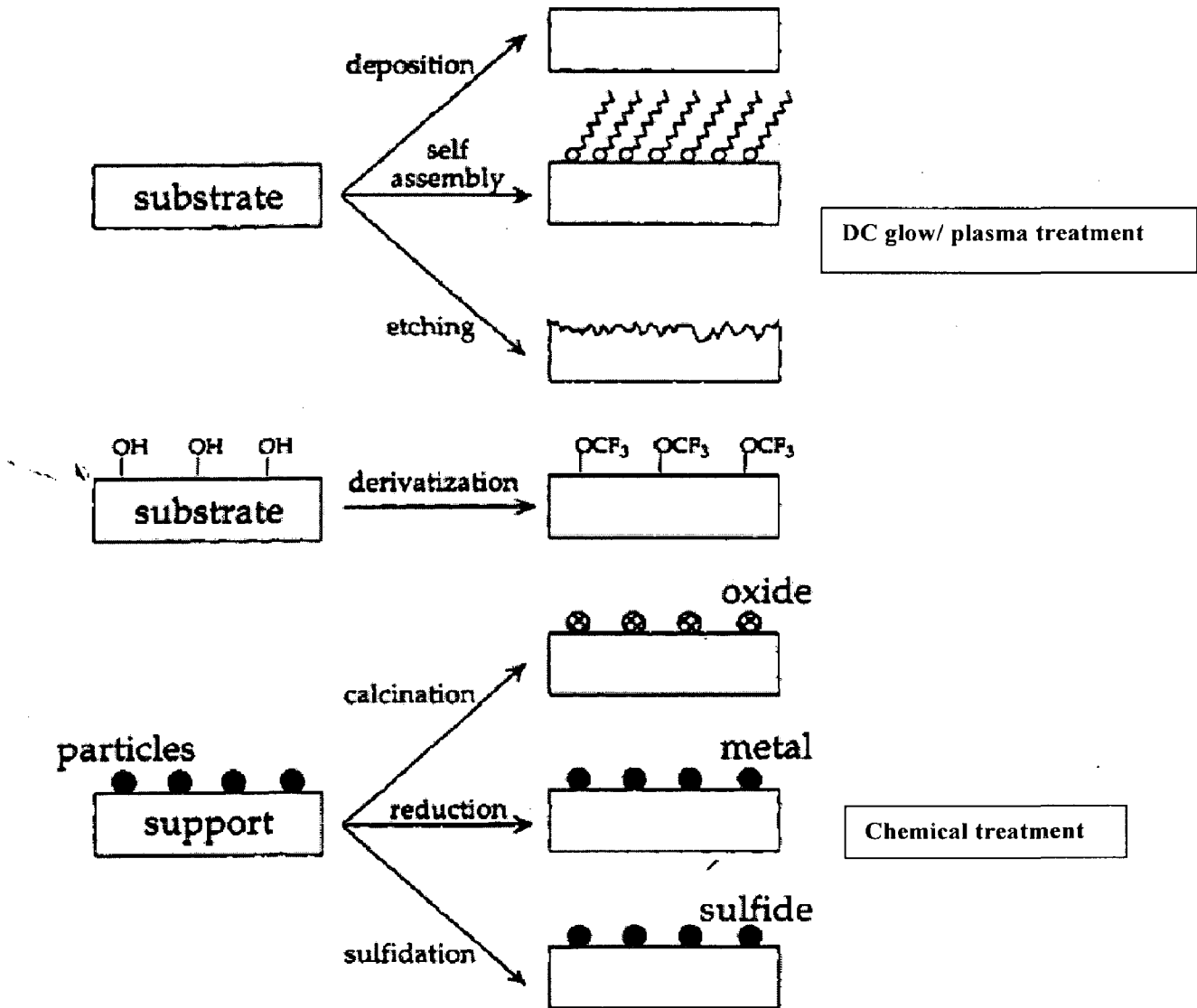
Fig. 1.7 Schematic representation of the surface modification methods: DC glow/plasma treatment and chemical treatment.

1.3.2 DC glow/plasma treatment

Plasma treatment has high intensity of highly enriched functional species at the surface results to formation of fairly uniform in thickness over the whole surface and long lived (Fig. 1.7). Heat sensitive polymeric materials can be successfully treated by plasmas. Normally, Plasma treatments are used to improve wettability, printability, sealability, and adhesion properties of polymers as well as to enhance polymer resistance to mechanical failure. These treatments are also employed to deposit thin polymer films on polymer surfaces or other packaging materials such as metals and glass [15]. In this treatment modifications are limited to the surface layer to a depth of typically 0.005 to 0.05 μm. Three dimensional objects can be treated without any difficulty by plasma processes and plasma surface treatments are friendly to the environment [15, 16].

1.3.3 Laser irradiation

Excimer laser provides UV light of short burst of high intensity which results photo-decomposition by direct chemical bond scission in the top layer of material. Excimer laser radiation has been used to substantially modify the surfaces of polymer as well as cleaning the surface of contaminants. These lasers has been used to create highly irregular microscopic structures on the polymeric surface that are useful for improving adhesive bonding, surface friction and in fabricating filtration, catalytic, field-emission cathode and light-trap devices. It can also change the charge state of a surface that is useful for surface wettability [11]. It is also used to substantially modified metal and semiconductor surfaces to remove oxide layers, clean, anneal and smooth them and improve their wear and corrosive properties.

1.3.4 Electron beam irradiation

Electron beam provides large amount of energy to the atoms of its path. It losses energy by collision with the electron of the atoms of target material results the chain scission in the polymer material and liberation of volatile product. This makes the target material surface highly reactive due to presence of free radicals and due to low penetration. It is used in lithography and for surface modification [12].

1.3.5 Ion beam irradiation

For most plastic materials, equivalent surface modification may be obtained by the use of either chemical; laser, plasma or ion irradiation cross linking, but ion irradiation may have the following advantages:

1. Irradiation has no lower limit on physical size, smaller conductor sizes.

2. Irradiation does not use high temperature or pressure. Separator tapes are not required to prevent thin wall insulations from being forced into the conductor strand surface.

3. Irradiation offers the insulation compounder design freedom. Compound additives may be chosen without regard to their reaction to high temperatures and to moisture.

1.4 Ion beam induced modification of polymer

The first experiment of the interaction of ion with solid were done and formulated by Rutherford. Ion beam irradiation/ implantation depends on the ion beam energy, fluence, angle of descend and ion specie. Each type of ion has indusial impression on material. In case of low energy (KeV) ions get embedded inside the material and cause modification by their presence and impinging ions produced by its collision cascade. On another hand in swift heavy ion (SHI)

irradiation, the modification of thin films or the surface or subsurface of bulk samples is due to the electronic excitation, not due to impinging ions produced by it, because they come out due to their large range. That's why it is better use for films, to understanding of interaction of it with matter.

1.4.1 Energy loss mechanism

By principle when ion passes through the material, the energy of the ion is losses by two collision mechanism − electronic and nuclear collision. The energy loss of these charge particles per unit length is defined as "stopping power", which varies material to material and usually written as:

$$S(E) = -(dE/dx)$$

Where E is the energy and x is the path length. The minus sign of expression is to present the loss of energy of charged particles as length increases. The energy loss can be expressed in terms of LET (Linear Energy Transfer) which measure the energy deposited per unit ion path length, often represent in SI unit of eV/nm. The magnitude of ionization depends upon the deposited energy along the ion track or energy deposited per unit path length [17].These energy depends upon electronic and nuclear stopping power.

Electronic stopping power: In this stopping, the charge particle (ion or electron) slow down due to the inelastic collision between bound electrons in the medium. Since the number of collision that an ion experiences with electrons is large and the charge state of ion while traversing the medium may change frequently. $S_e(E)$ is an average taken over all energy loss processes for different charge states. It is prominent in case of higher energy ions, as described by Fig. 1.9.

12
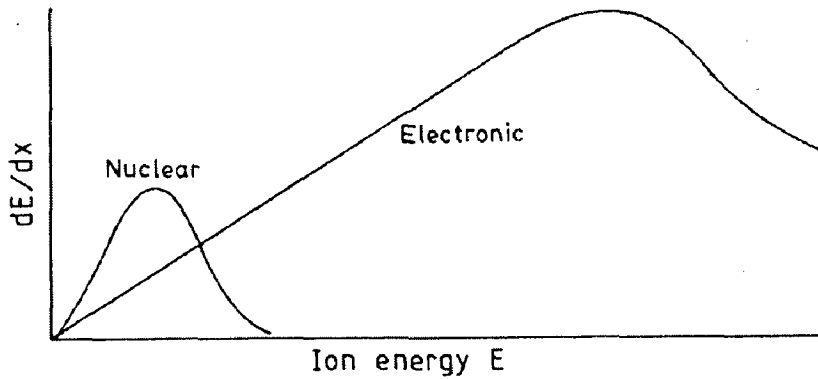
Fig. 1.9 Comparision of electronic and nuclear stopping at different energy range

Nuclear Stopping power: In this stopping, ions lose their energy by elastic collisions between the ion and atoms in the sample. It is prominent in case of low energy ions as clear from Fig. 1.9 and increases with the mass of ion.

At intermediate energies, the stopping power is therefore the sum of these two terms:

$$dE/dx = (dE/dx)_n + (dE/dx)_e$$
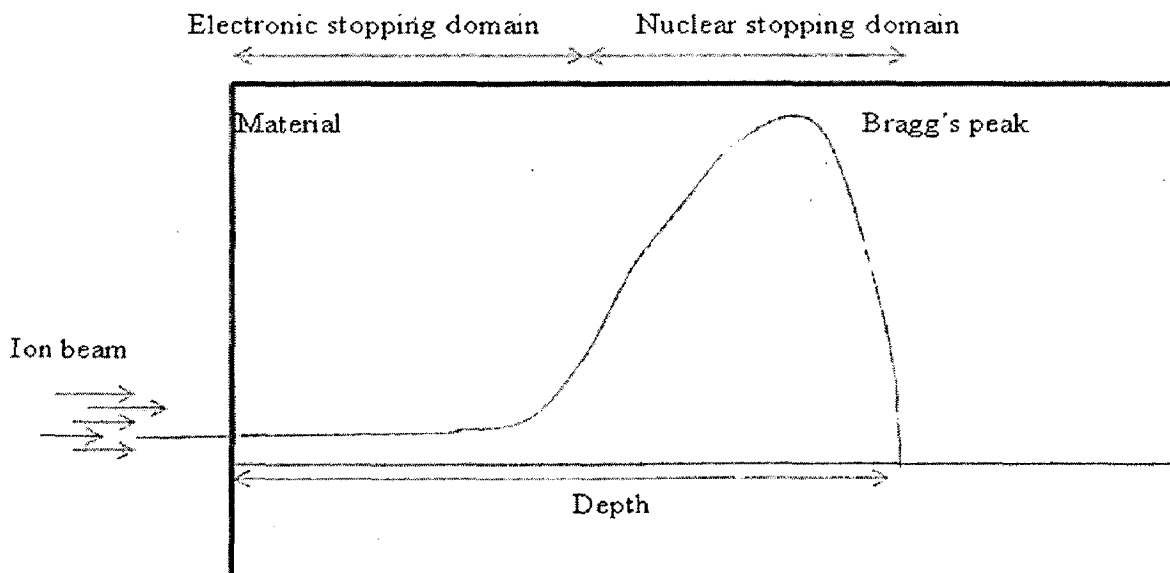
Fig. 1.10 Interaction of ion beam with target material

13

As shown in Fig. 1.10, in the beginning of the penetration depth, high energy of ion is slow down mainly due to the electronic stopping processes and it moves almost straight. As the ion slow down sufficiently, the nuclear stopping power become more effective, results an atom of target material receive significant recoil energies to remove from their lattice position and produce a cascade on further collisions which cause damage in material.

1.4.2 Types of ion beam used in irradiation

1- Proton beam-

    - low charge state ion beam

        ➢ with low energy (KeV) [18-22]

        ➢ with high energy (MeV) [23-26]

    - high charge state ion beam

        ➢ with low energy (KeV)

        ➢ with high energy (MeV) [27-29]

2- Cluster gas ion beam [30, 31]

3- Polyatomic ion beam [32, 33]

1.4.3 Types of modification using ion beam

As an energetic ion penetrates a polymer material, the material along the trajectory of ion beam modified, that is due to the breaking of atomic bonds and the rearrangements of polymer structure around the ion path result in a heavily modified cylindrical area, which is called latent track [34, 35]. The energy deposited along the ion path is extremely high and can reach several hundred eV/Å which is sufficient to break the all bonds in the track core such as C-H, C=C, C=O etc. In this way, the tracks of energetic ions can be used to modify the physical and chemical properties of polymers [36, 37].
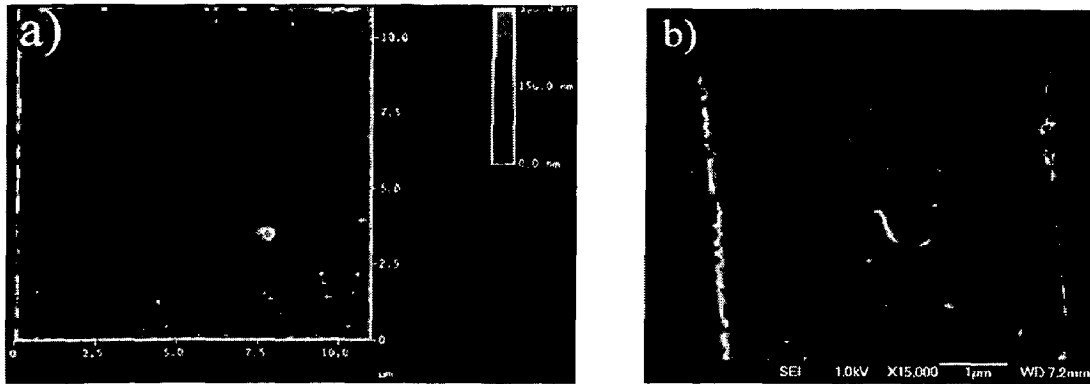
Fig. 1.11 Examples of (a) an AFM image of a square exposed to a dose of 40 nC/mm^2 and (b) a low voltage SEM photo of a square exposed to a dose of 120 nC/mm^2, both samples were dip developed for 4 min. [38]

The physicochemical modification during ion implantation was due to following mechanism takes place along the ion path in organic polymers-

1- Cross-linking

2- Chain scission

3- Gas liberation

4- Change in crystallinity

Cross-linking and chain scission are result of reactions take place during high energy ion irradiation on polymer surfaces [39, 40].

Cross-linking

When materials irradiate with ion, liberation of volatile product and radicals who produced on the neighboring polymer units, that leads to the formation of interlink bond, called cross linking (Fig. 1.12). The relative molecular mass of the macromolecule increases which resulted in an increase of melting point.
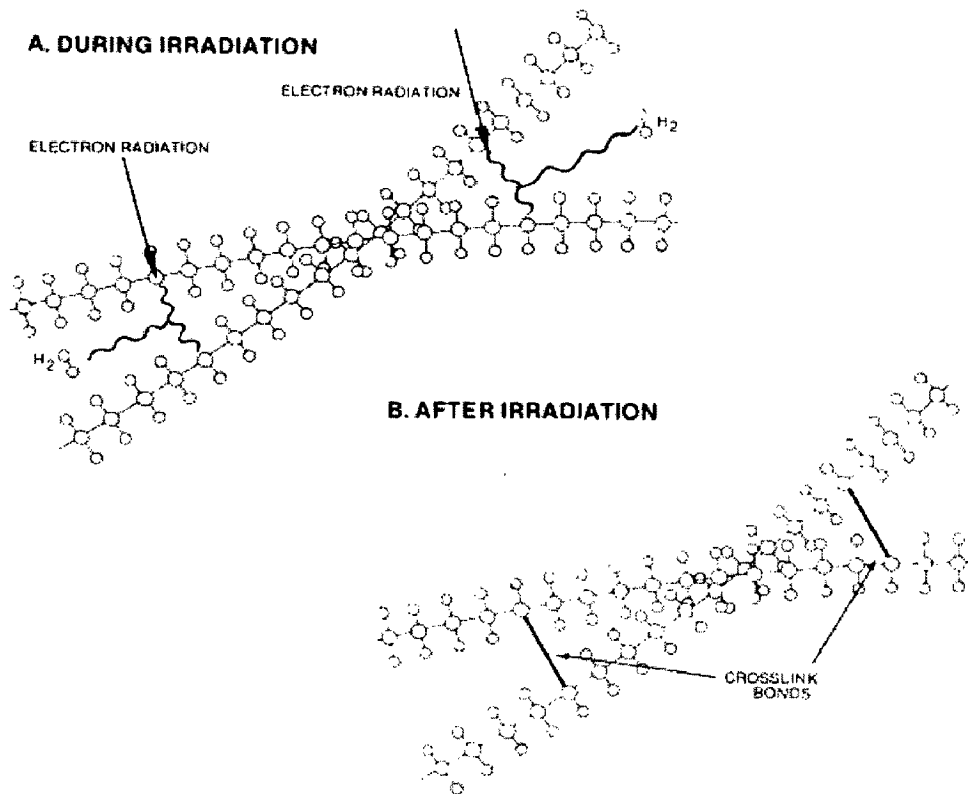
Fig. 1.12 Two random polyethylene molecule during and after irradiation cross-linking.

Cross-linking provides higher tensile strength, improved fluid resistance, better crush resistance, solder iron resistance, change in thermal stability, better over load characteristics, change in flexibility, resistance to stress cracking, improved high temperature mechanicals

Chain scission

When ion beam irradiate on polymer, degradation takes place by chain scission which leads to a decrease in the molecular mass. Low-fluence hyper-thermal ion implantation of ions such as Ar^+, He^+ and H^+ causes scission, while higher doses of such ions usually creates cross-linking [41]. It was also reported that cross-linking or scissioning efficiency depends not only on polymer structure but also on the characteristics of the radiation sources, namely ion energy and ion specie. For example, in case of low fluences, PMMA undergoes chain scission and opposite to

this polystyrene follows cross-linking [24-26]. Thus, fluence dependency of chain scission and cross linking makes interesting to the PMMA because it has been reported that beyond a given threshold fluence the PMMA resist turns negative due to the scission rate [42].

Gas liberation

As ion beam irradiation interact directly to the target material, it causes bond scission, ablation due to its energy, results the rapid chemical decomposition of material, which produces small molecular fragments such as CO, CO_2, CH_4, CH_3OH and $HCO-OCH_3$ [43].

Change in crystallinity

In general Ion beam irradiation produces crystallinity in case of metal and semiconductor higher as compared to insulators such as polymers. But experiments showed that semi crystalline polymers are also amorphous after irradiation by suitable ions [44], resulting from scission process of the main chains. The processes such as chain scission, cross-linking, etc. were observed to be highly dependent on the fluence and the energy of ions. Thus change in crystallinity depends on fluence. For example, C^{5+} ion beam of energy 70MeV results decrease in crystallite size by 8% than un irradiated PMMA at fluence 1.2×10^{14} [45].

1.5 Improvement in polymeric material properties due to ion beam irradiation

Modification of polymer properties under ion radiation is a subject of widespread importance due to the increasing use of polymeric materials in hard radiation environment such as:

1- Space application

2- High energy physics experiments

3- Nuclear power plants

4- Sterilization irradiators

The application of radiation on polymers can be used in various industrial sectors such as biomedical, textile, electrical, membrane, cement, coating, rubber goods, tires and wheels, foam, footwear, printing rolls, aerospace and pharmaceutical industries [46]. When polymeric materials are used for such application, a detail study of different type of radiation effect must be done. Such can be done by using different type of ion beam irradiation. Due to this ion beam irradiation have a vital role in field of research in science & technology. Ion beam irradiation provides a unique way to modify polymers properties such as mechanical, optical and electrical by depositing the energy of ions in the material on atomic scale results from the changes of the chemical structure caused by changing the chemical bonding when the incident ion breaks the polymer chain & covalent bonds, promotes cross-linking and liberates certain volatile specie [43] which depends on the properties of the polymer, such as the composition and molecular weight, and on the mass and energy of the incident ions, as well as on the conditions of irradiation. Therefore the structural rearrangement influences the properties of the polymeric materials and opens a new way to design devices with required parameters.

1.5.1 Dielectric properties and its improvement

Dielectric materials are the building blocks of fundamental electronic circuits, capacitors, gate dielectrics and transmission lines, are essential as electrical insulators for power distribution [47]. The dielectric properties of materials are used to describe electrical energy storage, dissipation and energy transfer. Electrical storage is the result of dielectric polarization. The two important mechanisms that results the molecular polarisability are: 1- Distortional polarisability

2- Orientational polarisability

In distortional polarisability, the applied electric field changes the electric charge distribution and induces an electric dipole moment, leading to a contribution.

In orientational polarisability, the external electric field applied to the materials which have permanent electric dipoles even in absence of any electric field, the molecules tends to rotate so that the dipoles become aligned with the field the direction.

In polymers, the alternating current frequency is an important factor because of the time dependence of polarization of dipoles. At very low frequencies the dipoles have sufficient time to align with the electric field before it changes its direction and resulting dielectric constant is usually high. At very high frequencies, the dipoles do not have time to align before the field changes its direction, results the lower dielectric constant. Dielectric constant/loss increases with increasing fluence which is associated with electron transition.

1.5.3 Optical properties and its improvement

PMMA is highly transparent that's why used as glass and due to hardness and elastic properties, used in goods. The use of polymers is increases day by day owing to their strength to weight ratio, lower cost, and lightness and have excellent optical properties. Interestingly ion beam modification improved the optical properties of various polymeric materials due to degradation [6, 19, 20, 27]. The understanding of certain structural re-arrangements influence on the suitable properties of polymers opens a way to design devices with required parameters, involving such applications as optical filters, absorbers, reflectors, luminescent devices etc. [48]. The optical properties of ion implanted polymers, being of particular interest for modern optoelectronics and photonics, have been extensively explored [24, 25, 49].

1.6 Irradiation with high charge state ion

The functional definition of a 'highly charged ion' (HCI) is an atom that has been stripped of a large number of electrons ($Q > 1$), so that the total energy yielded during reneutralization (E_0) is outside the realm of ordinary experience with laboratory ions ($E_0 >> 10$ eV) [50]. These are also called hollow atoms due to empty of inner shells of atoms in case of high charge state ions.

HCIs potential energy is the sum of the binding energies of all ionized electrons. This potential energy also referred to as neutralization energy. It is reported that slow HCIs, ions where the potential energy exceeds their kinetic energy (e.g. Xe^{44+}), can produce near surface structures in the nanometer length scale [1, 51]. Due to their low kinetic energy, slow HCIs do not penetrate into the deeper layers of the solid. Thus it is expected that HCIs open up new possibilities for surface modification and its application.

In case of highly charged states ions, in the conventional ions kinetic energy range, the relative importance of kinetic energy to potential energy is reduced, or inverted sometimes by a large factor because its potential energy is very high than the kinetic energy. As high charge state ions inters into the material due to de-acceleration it produces photon energy thus inside the material it energy is composed of three energies namely; kinetic energy, potential energy and photon energy.

Ultra-slow HCIs is the minimum impact velocity (v_m) of an ion under the influence of unscreened image charge acceleration by a surface. If one tries to perform an experiment by directing an ion beam onto a surface with velocity $v < v_m$, the ions will automatically accelerate to v_m shortly before impact. For very highly charged ions, v_m can be surprisingly close to the crossover velocity.

1.6.2 Interaction of low energy and high charge state ions with surface

As the HCIs reach the target surface, due to their great electrostatic pull electrons begins removing from highly localized region of the surface even when it is tens of atomic diameters away which are estimated to be on the order of 1–10 nm in diameter [1]. Numbers of the removed electrons that are swing around the ion and then travel back to the target surface not necessarily landing back at their origin of point because of the dynamical evolution of the ion–surface system in the meantime. In addition, some of the electrons are captured temporarily by the ion and become bound in high-lying Rydberg levels. This forms a so-called 'hollow atom' [51] in which most or all of the electrons are in an excited state.

Normal Na: 1s2, 2s2, 2p6, 3s

Hollow Na: 1s0, 2s0, 2p3, 3s1

Inner shells empty

Fig. 1.16 simple representation of hollow atom for example Na^{7+}

The population of high-lying levels (in a hollow atom) can subsequently decay to lower levels gives up either a photon or a secondary electron (Fig.1.16). At this stage of HCI, the decay proceeds most rapidly through interaction with other bound electrons in an Auger process. Through which the partially neutralized ion automatically recognizes itself, as it continues to approach the surface. Some parts of this Auger emitted electrons are directed back towards the surface in a diffuse beam, and parts are ejected outwards away from the surface where they can be readily detected. In addition, the experimental observations of several hundred electrons have been measured to be projected away from a surface by a single low velocity HCI. Thus, HCI acts

21

like a miniature electron pump to remove a large number of electrons from a nanometer-sized region of the surface in the femto-second range.

1.6.3 Importance of high charge ion in nanotechnology

In view of the availability of low energy HCIs in India as well as in other country, open a major area for the development of new techniques in the area of nanotechnology because these ion beams may be also widely used in the fabrication of microelectronic devices of unique characteristic which might not be achieved by conventional ion beam. Particularly slow HCIs are interesting, that can be produced with small and inexpensive devices and produced nanostructures on surface or subsurface region.

The key step in microelectronics fabrication is lithography in which charged particle ion beam focusing and rastering can be effectively applied to high-Z and/or high-Q ions [52]. Slow HCIs need only a nanometer range mask to produced surface feature, and the electrons captured by an HCI during edge scattering will tend to neutralize it. During this case of HCI a tremendous amount of potential energy seems to be deposited in the first few atomic layers near the surface, and the kinetic energy seems to be largely irrelevant. The physical picture obtained during mica is emerging suggests that individual HCIs can produce fundamentally uniform nano-scale structures even in the limit that the ion energy is reduced towards zero [1]. Thus, slow HCIs have important implications for lithographic patterning of shallow-junction devices, surface modification, and other cases in which deep ion damage to the underlying substrate must be avoided

CHAPTER 2 LITERATURE REVIEW

2.1 Background

In recent years, the modification of organic polymeric materials using energetic ion beams has become a wide field of basic research, especially regarding the underlying processes of damage creation. Ion beam technique is widely used as a flexible and powerful tool for different materials surface engineering, including polymers. The in the ion implantation of polymer materials is due to the possibility of precise control of the technological parameters for fundamental research purposes, and also considering some possible applications to device fabrication such as, grating, diffractive structures, optical waveguide, etc.[24, 25]. As well as surface modification of polymeric materials [19, 27, 53-55] by ion beam irradiation/implantation also increased attention due to possibility of controlled modification, even in atomic layer order on controlling the technological parameter, ion energy, ion nature, and also considerable possibility of applications such as optical filters, absorbers, reflectors [56] and increase the wettibility for biological applications [7-11, 57].

Polymer materials (e.g. PMMA, PC, etc) are currently used extensively because of their excellent materials properties, like high optical clarity, low attenuation and weathering ability, the good tensile strength and hardness, high rigidity, good insulation properties and thermal stability dependent on tactility, etc., and are interesting for their optoelectronic properties. Such type attractive materials properties of PMMA, combined with relatively low cost of production, have led to their widespread use in the manufacture of microwave, electronic and photonic systems [58]. For application of surface of PMMA, thermal and hyper-thermal surface

modification of PMMA has been previously done computationally [59-61] and experimentally [62, 63].

PMMA have some disadvantages also such as brittleness and low chemical resistance which can be eliminated by chemical or physical modification such as laser, plasma and ion beam. PMMA contains both hydrophobic (methylene) and hydrophilic (carbonyl) groups in each unit [58]. Most polymeric surfaces as well as PMMA are inert, hydrophobic in nature and usually have a low surface energy, and do not possess required specific surface properties needed in various applications [64, 65]. In such case, there is a possibility of selective modification of the surface, with keeping bulk characteristics unchanged, has greatly increased the applicability of polymers [66] that could be also obtained by low energy and high charge state ion beam irradiation[67].

Ion implanted with sufficiently large ion dose in the range 10^{15}–10^{17} Si^+ per cm^2 PMMA have higher reflectivity and diffused reflectivity as compared to the non-implanted PMMA, due to the structural modification of the subsurface region of PMMA which may be results of practical interest for the ophthalmic intraocular lenses, diffractive optic elements and micro-components for integrated optical circuits based on ion implanted PMMA [68].

The optical absorption of Si+ ion of energy 30 & 50 KeV implanted PMMA can be manipulated, both in the visible and the IR range, depending on the ion dose [20]. This could be due to an increased of defect above some critical concentration causing an abrupt increase of structural disorder. Thus, these can be used for optoelectronics and photonics [20].

It is reported that PMMA layer maximum damage at smaller angles (< 60°) and almost no damage at or close to 90°, which show that damage in PMMA is due to formation of bubbles and holes [23].

The gas cluster ion beam (GCIB), which consists of several thousands of atoms, and Polyatomic ion beams, such as C60, has been also used for surface modification and analysis of inorganic and organic materials such as Leucine, Arginine, PC, PS and PMMA [31, 33].

2.2 Aim and scope

Low energy with high charge state ions plays an important role in surface or subsurface modification because the potential energy HCIs exceeds their kinetic energy. Therefore it can produce surface modification or surface structures in the nanometer length scale [1, 68]. The nanometer range surface modification determines the most important properties of new materials.

Therefore, with the availability of such kind of high charge ion beam of low energy, it would be interesting to study their effect on nature of modification of polymeric surface. We present here some important result of our experiment based on low energy with high charge state Oxygen and Nitrogen ion beam irradiation on PMMA using ion implantation facility based on ECR technique available at VECC Kolkata shown in Fig. 3.3.

In such way high chare state ion beam facility working at room temperature provides a lot of advantages in device fabrication, such as a device very small compared to cryogenic devices, transportable, lab on chip, very simple to operate and both initial and maintenance costs are much lower.
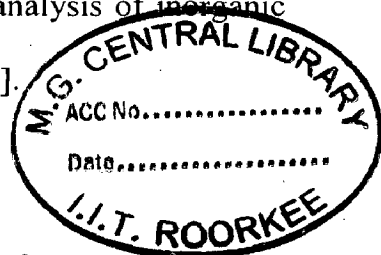
CHAPTER 3

EXPERIMENTAL AND CHARACTERIZATION TECHNIQUE

This chapter deals with experimental technique (ECR ion source), that used during experiment and characterization technique UV-Vis-NIR spectroscopy, dielectric constant, FE-SEM.

3.1 Electron cyclotron resonance (ECR) ion source principle and its operation

When electrons move in a magnetic field they gyrate around the magnetic field lines due to the Lorentz force. The gyration frequency is called the cyclotron frequency ω_{cyc}. If microwave radiation of the same frequency propagates into such a region, the electrons are resonantly accelerated or decelerated (depending on the phase of their transversal velocity component with respect to the electric field vector) when the electron cyclotron resonance condition is fulfilled:

$$\omega_{rf} = \omega_{cyc} = (e/m)\ \omega\ B$$

Here, e and m denote the charge and mass of the electron, respectively. The plasma electrons are confined in a superposition of an axial magnetic field component (produced by solenoids or permanent magnets) and the radial magnetic field of a multipole magnet. This result in a so-called minimum-B-structure Fig.3.2 because the magnetic field has a minimum in the middle of the structure and from there increases in all directions. Therefore, a closed surface is created where the electron cyclotron resonance condition is fulfilled. Electrons passing through that surface can be accelerated resonantly. Furthermore, a high mirror ratio of the magnetic field leads to long confinement times for the plasma electrons. They can pass the resonance region very often, gain high energies and ionize plasma atoms and ions into high charge states via successive single ionization.

26
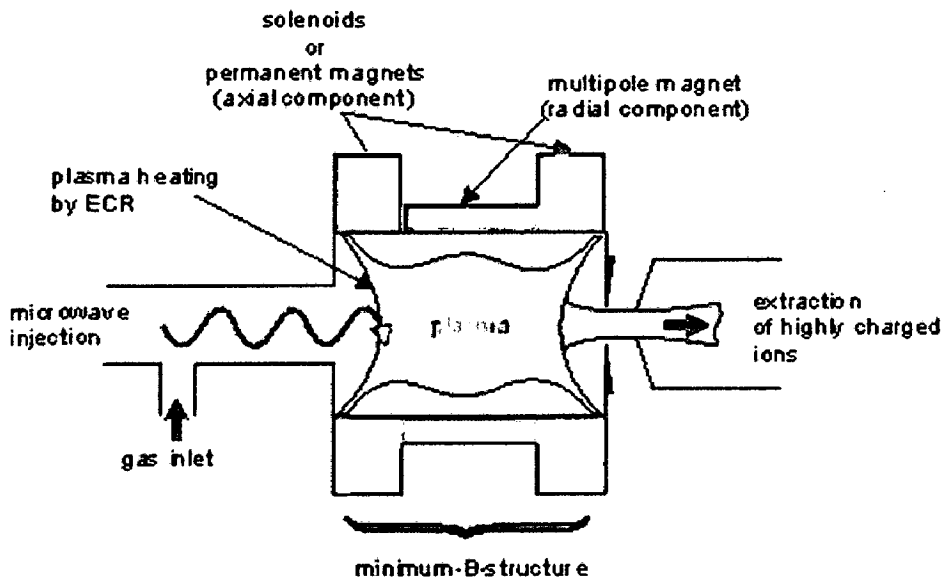
Fig. 3.1 Schematic diagram of an ECR ion source
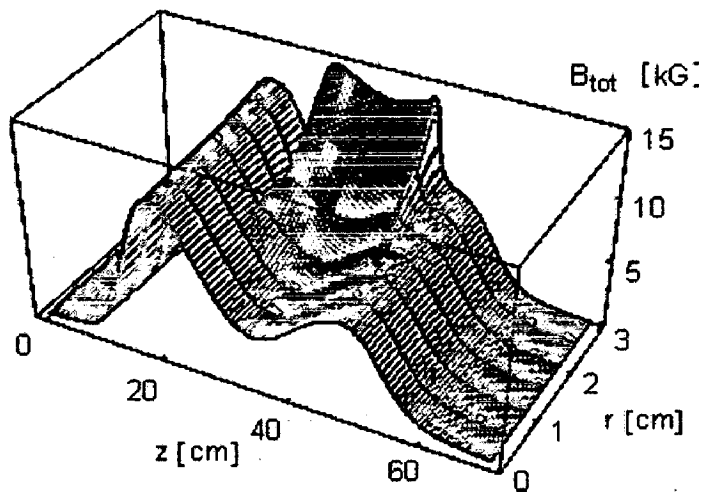
Fig. 3.2 Magnetic field of a minimum-B-structure for a 14 GHz ECRIS

The ions in the plasma are not accelerated due to their large mass and remain thermal. Therefore they are confined by the space charge potential of the electrons, but not by the magnetic field.

This magnetic confinement, however, is not perfect and electrons can leave the plasma, for example in axial direction. Since the plasma tends to stay neutral, ions will follow the electrons. By using suitable extraction geometry and by applying a high voltage, the ions are extracted from the ion source.

(a)

ANALYZING
MAGNET

OBJECT
SLIT

IMAGE
SLIT

QUADRUPOLE
TRIPLET

GLAZER
LENS

SAMPLE
CHAMBER

ECR
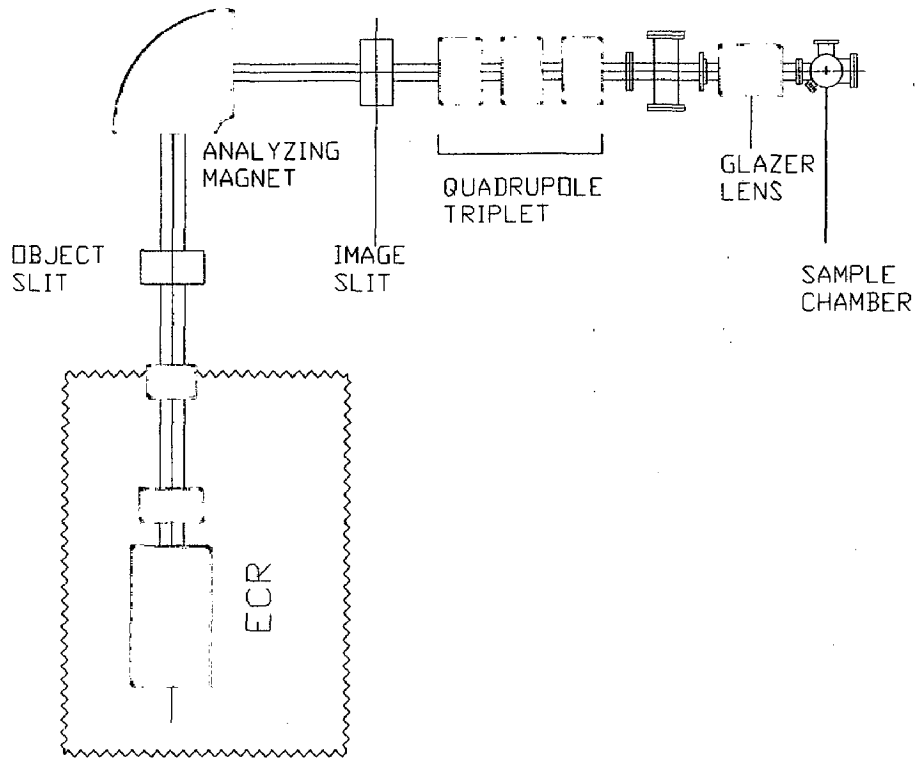
(b)

Fig. 3.3 Schematic diagram (a) and Complete picture of ECR (b) Low Energy Ion Implantation setup at VECC Kolkata.

28

After extraction ions are separated by a 90 degree analysing magnet and detected at the end of the analysing magnet by Faraday cup. The ion pulse charges collected at the Faraday cup can be measured both separately and cumulatively using a high-precision Ampere meter. The kinetic energy of the ions at the target which is at ground potential is determined by the product of the charge and the potential called trap potential [69]. This potential is in the order of some keV depending on the chosen electron beam energy which determines the ionization energy in the trap. In order to obtain high kinetic energies for high charge state ions, the sample are floated at required negative voltage.

3.2 UV-Vis- NIR spectroscopy

Ultraviolet, visible and near infra red spectroscopy is the measurement of the attenuation of beam of light after it passes through a sample or after reflection from a sample surface. Absorption measurements can be at a particular wavelength or a range of wavelength (spectral range). UV- Vis light is energetic enough to promote outer electron to higher energy levels. UV light have energy to hole transition. Near infra red spectroscopy deals with rotation of molecule. The UV–Vis spectroscopy is generally used for molecules or inorganic complexes in solution. The concentration of an analyst in solution can be determined by measuring the absorbance at some wavelength and applying Beer-Lambert Law,

$$A = -log10\left(\frac{I}{I0}\right) = cL\varepsilon$$

Where A, $I0$, I, c and L are measured absorbance, intensity of incident light at a given wavelength, transmitted intensity, concentration of absorbing specie and the path length through the sample.

Different molecules produced during ion implantation, absorb radiation of different wavelengths. An absorption spectrum will show a number of absorption bands corresponding to structural groups within the modified molecule. In a material, the molecule and atoms can rotate and vibrate with respect to each other. These vibrating and rotating molecules have discrete energy levels, which can be considered to be packed on top of energy level, having very small energy separation to each other. Therefore it will show spectrum in NIR region. Most organic compounds that absorb UV-Vis radiation contain conjugated pi-bonds.
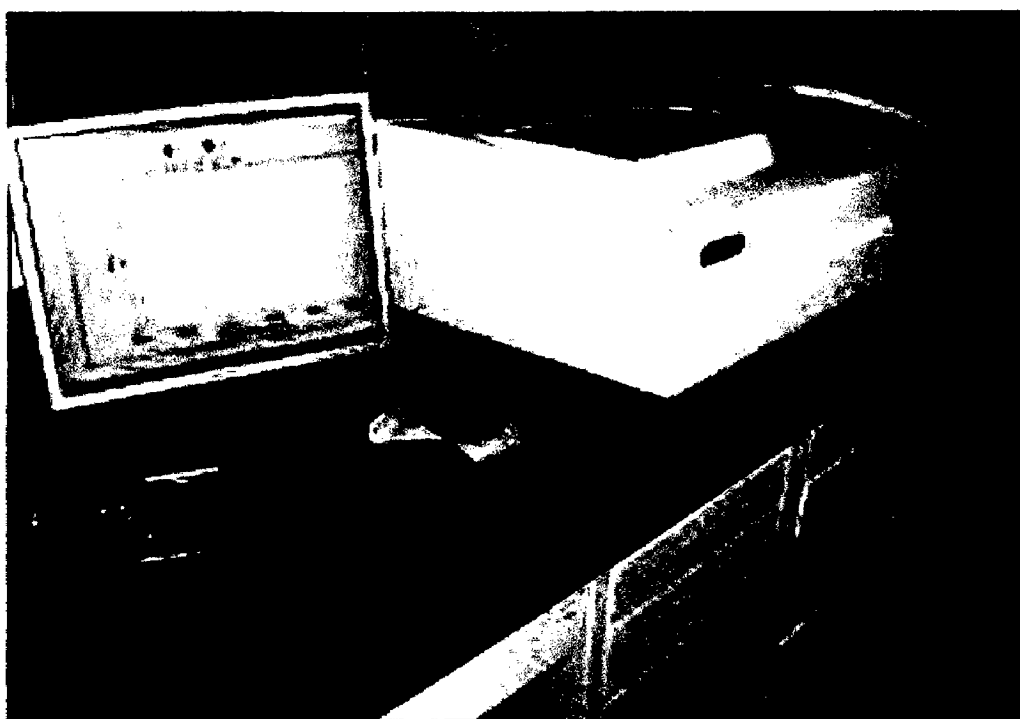
Fig. 3.4 Picture of UV-Vis-NIR spectrophotometer (Varian Carry 5000)

UV, Vis-NIR spectrophotometer works in wavelength range of 200-2500 nm shown in Fig. 3.4. The dual-beam deign spectrophotometer simultaneously measure absorption/transmittance coefficient spectrum of the sample and reference cells. In UV-Vis-NIR spectrophotometer,

mirrored rotating chopper wheel use to alternatively direct the light beam through the sample and reference cells.
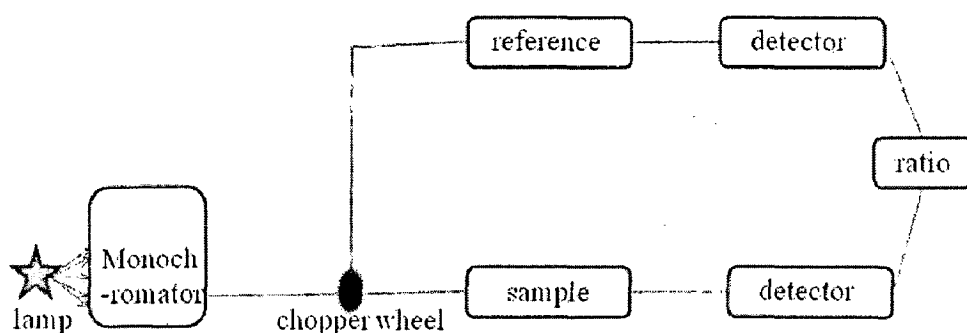
Fig. 3.5 Schematic diagram of a dual-beam UV-Vis-NIR spectrophotometer

The detection electronics or software program is then to manipulate this coefficient values as the wavelength scans to produce the spectrum of absorbance or transmittance as a function of wavelength. It measures the intensity of light passing through a sample and compares it to the intensity of light before it passing through the sample as shown in Fig. 3.5. The ratio is called the transmittance, and is usually expressed as a percentage (%T).

Irradiation of polymers results in shifting of absorption edge from UV towards the visible region. This shift can be correlated with the optical band gap by expression:

$$Eg = \frac{hc}{\lambda}$$

Optical characteristic of pristine and irradiated samples have been studied in wavelength range of 300-2500 nm by using UV-Vis-NIR spectrophotometer.

31

3.3 Dielectric measurement

In general, the atoms of polymer have their electrons, tightly bound to the central long chain and side groups through 'covalent bond'. Covalent bonding makes it much more difficult for most conventional polymers to support the movement of electrons and therefore they act as insulator.

Generally, the chemical bonds between unlike atoms in polymer molecules posses permanent electric dipole moments. Many polymers show polarization due to orientation of permanent dipoles in the presence of electric field. They are said to be 'dielectric active' polymer. The measurement of the polarization induced in dielectrically active polymers has proven to be an extremely useful method for probing polymer structure. Dielectric constant is an ability of the material to store electric charge through polarization.

Dielectric constant of pristine and irradiated polymer have been measured by LCR meter (Model 3532-50, HIOKI), which uses powerful microprocessor-controlled digital and analogue technique to provide a comprehensive range of temperature and frequency response measuring facility, and give directly values of capacitance, resistance and dielectric loss. It has working range from 100 Hz to 0.1 Hz.

3.3.1 Dielectric constant

Dielectric constant may be define by two way, 1- The property of a dielectric which determines the electrostatic energy stored per unit volume for unit potential, 2- The ratio of the capacity of a condenser having a dielectric material between the plates to that of the same condenser when dielectric is replaced by a vacuum as in Fig. 3.6.

Therefore $\varepsilon = Cp/C_o$, where Cp is capacitance measured in presence of dielectric material;

$C_o = \frac{\varepsilon_o A}{d}$, where ε_o is the permittivity of free space, A is the cross-sectional area of the electrode and d is the thickness of the polymer.
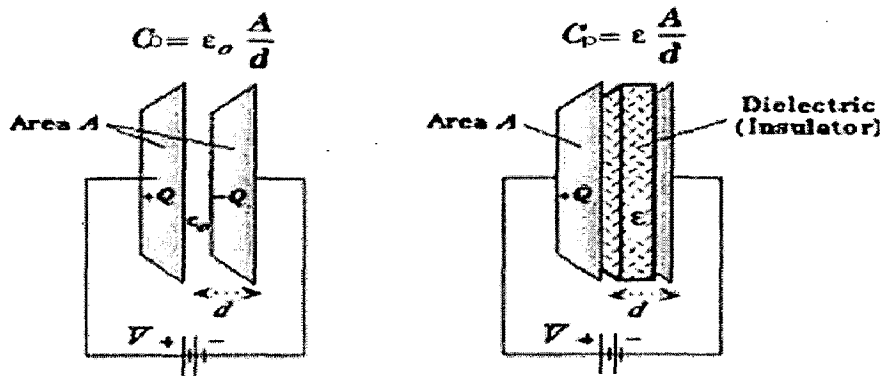
Fig. 3.6 Schematic diagram of principle of capacitance measurement

When dielectric material is inserted between the plates, and the electric field applied on it, the material being polarized in such a way that the material remains neutral but induced charge appears on the plates. The insertion of material between the plates of capacitor always increases its capacitance, because when the capacitor is filled with a material 'say' solid, liquid or gas, the induced charge increases the polarization of the medium as shown in Fig. 3.7.

$$Q = Q_o + P = \varepsilon_o(1 + \chi)E = \varepsilon$$

Where, ε is the permittivity and χ the susceptibility of the dielectric material.

33
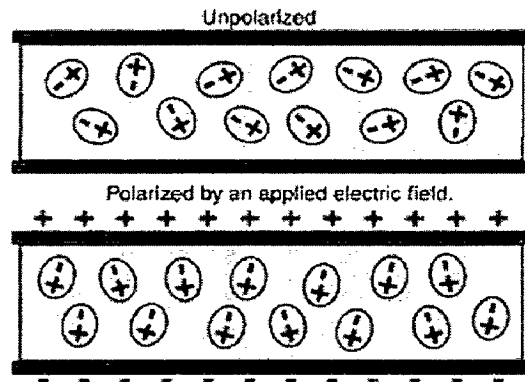
Fig. 3.7 Schematic diagram of unpolarized and polarized of dipole in absence and presence of electric field respectively

If all other factors remain unchanged, as the dielectric constant increases, the electric flux density increases. Materials with high dielectric constants are useful in the manufacture of high value capacitors.

Therefore dielectric constant ε determine by

$$\varepsilon = Cp. \frac{d}{\varepsilon_o A}$$

3.3.2 Dissipation factor/dielectric loss

It is a measure of the hysteresis in charging and discharging of dielectric material and simply loss in capacitance. The loss is the tangent of the phase angle relationship between capacitor voltage and capacitor current, which theoretically 90°. It is also represented by tanδ. It can also define as a measure of loss rate of power of a mechanical mode, such as an oscillation, in a dissipative system.

3.4 Field emission scanning electron microscopy (FE-SEM)

In the FE-SEM, the vacuum allows electron movement along the column without scattering and helps prevent discharges inside the instrument. The vacuum design is a function of the electron source due to its influence on the cathode emitter lifetime. The function of the electron gun is to provide a large and stable current in a small beam. There are two classes of emission source: thermionic emitter and field emitter. Emitter type is the main difference between the Scanning Electron Microscope (SEM) and the Field Emission Scanning Electron Microscope (FESEM).
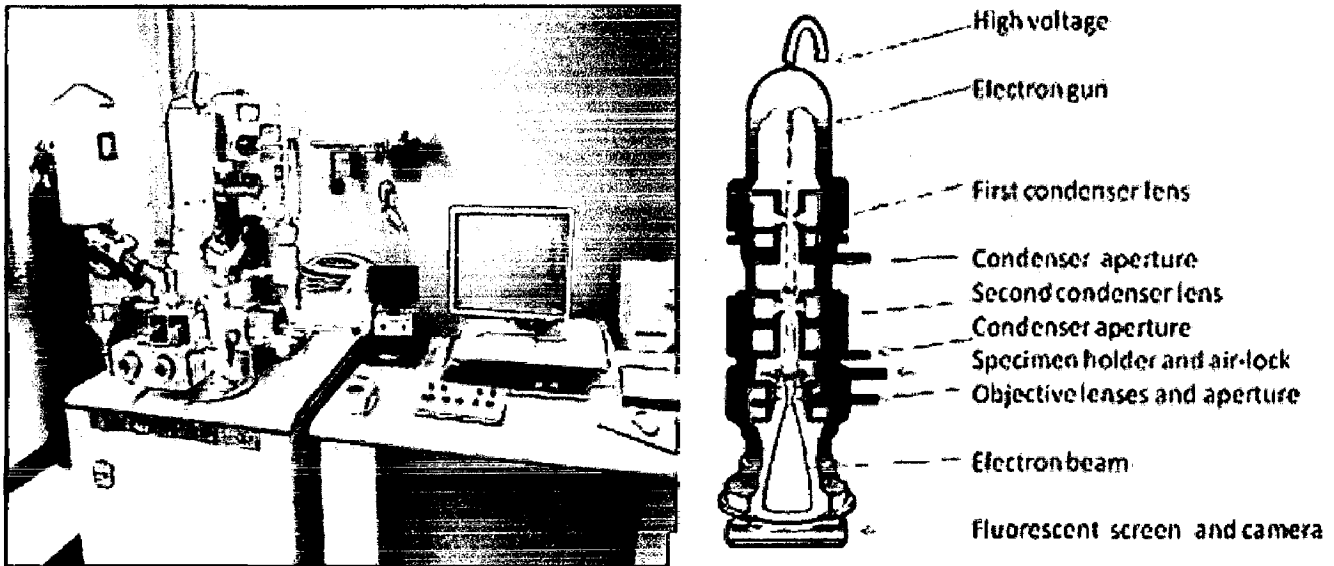
Fig. 3.8 Picture FE-SEM instrument and its working principle

Thermionic Emitters use electrical current to heat up a filament; the two most common materials used for filaments are Tungsten (W) and Lanthanum Hexaboride (LaB$_6$). When the heat is enough to overcome the work function of the filament material, the electrons can escape from the material.
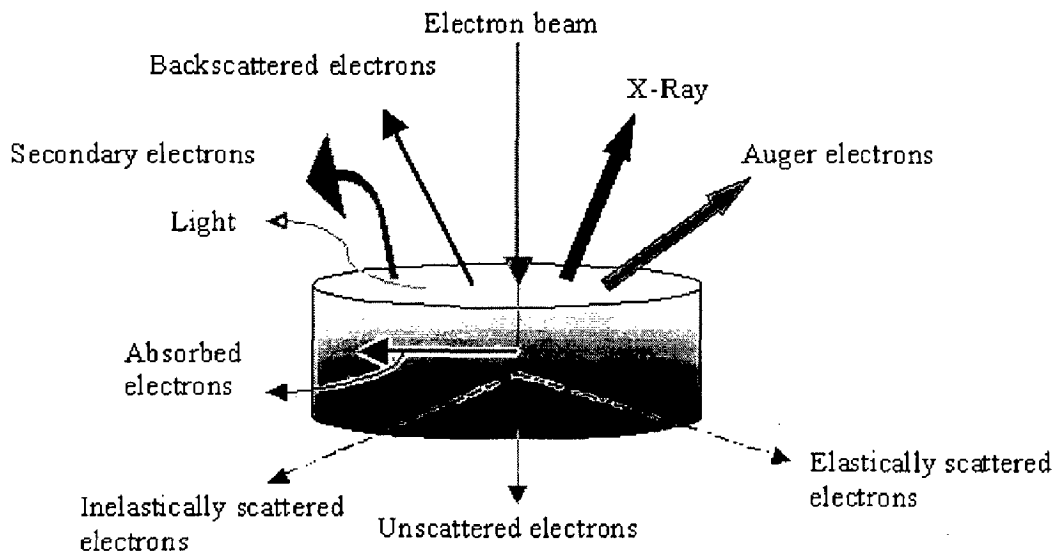
Fig. 3.9 The generation of different type of electrons during electron beam interaction with material

Field Emission is one way of generating electrons that avoids thermionic emitter's problems such as low brightness, evaporation of cathode material and thermal drift during operation. A Field Emission Source (FES); also called a cold cathode field emitter, does not heat the filament. The emission is reached by placing the filament in a huge electrical potential gradient. The FES is usually a wire of Tungsten (W) fashioned into a sharp point. The significance of the small tip radius (~ 100 nm) is that an electric field can be concentrated to an extreme level, becoming so big that the work function of the material is lowered and electrons can leave the cathode.

To resolves a feature on the specimen surface, the beam diameter must be smaller than the feature. Therefore, it is necessary to condense the electron beam. To assist in the demagnification of the beam, electromagnetic lenses are employed. Small objective aperture sizes will produce better resolution, good depth of field and minimal charging.

The specimen and the electron beam interact in both elastic and inelastic fashion giving different types of signal. Elastic scattering events are those that do not affect the kinetic energy of the electron even when its trajectory had been affected. Inelastic scattering events are a result of the energy transference from the electron beam to the atoms in the specimen, as result the electrons have energy loss with small trajectory deviation. Some of the signals created in this way are: secondary electrons (SE), Auger electrons and X-Rays as shown in Fig. 3.9.

In the present study, the surface morphology of the irradiated and pristine PMMA was analyzed by FETQUANTA-200F field emission scanning electron microscope having an accelerating voltage of 30 kV.

CHAPTER 4

EFFECT OF 2+ & 7+ CHARGE STATE OXYGEN ION BEAM IMPLANTATION ON PMMA (POLYMETHYL METHACRYLATE)

4.1 Experimental

Commercially available PMMA (polymethyl methacrylate) sheet (Goodfellow, UK) of thickness 1 mm was used to study in present study. The samples were cut from sheet of size $10 \times 10 \ mm^{-2}$.

These samples were cleaned with propanol-2 and hand polished. So that small scratches were readily polished. These samples were irradiated with high charge state Oxygen ions beam (O^{2+} & O^{7+}) at accelerating energy of 63 KeV under identical conditions, using a low energy ion implantation facility developed at VECC Kolkata which was based on ECR ion source. The as-extracted beam of O^{7+}, having energy of 63keV, was used to implant one set of samples. During implantation with O^{2+} beam the sample was floated at a negative high voltage of 22.5kV to get total beam energy of 63keV. The ion beam was scanned over $10 \times 10 \ mm^2$ area of the sample using X-Y magnetic beam scanner. The particle doses of O^{2+} and O^{7+} beams were $1.4x \ 10^{17}$ and 1.0×10^{16} particles/cm^2 respectively with a beam current of about 1 μA.

Total reflectivity and absorbance data for the high charge state Oxygen ions implanted PMMA samples were obtained at near-normal incidence (≈ 3°) by Varian Carry 5000 UV–vis-NIR spectrophotometer. The spectra were recorded over the wavelength range 300–2500 nm using the above instrument equipped. The pristine PMMA was used for reference reflectance and absorbance material, So that the results show the enhancement in properties due to ion implantation. All samples were measured under identical conditions at room temperature. The transmittance data was obtained at normal incidence in the wavelength range 300-2500 nm. The

dielectric responses of the implanted and pristine PMMA samples coated with thin film of silver paste were measured in capacitor mode (as described in Chapter-2) at room temperature in the frequency range 300 Hz–0.1 MHz by LCR meter (Model 3532-50, HIOKI).

The surface morphology of the irradiated and pristine PMMA was analyzed by FETQUANTA-200F field emission scanning electron microscope having at accelerating voltage of 5 kV. The elemental analysis of these samples was performed using an EDXA accessory equipped with a charge coupled device camera.

4.2 Results and discussion

The simulated spatial distribution (range) of 63keV oxygen ion beam in PMMA is given in Fig.4.1 from SRIM calculation [70] and the end of range was ~360 nm. The implanted samples appeared brown in colour. Low energy ion implantation of PMMA is expected to modify the material via (side) chain scission. In addition, it could lead to defects via formation of voids due to nuclear energy loss, which is predominant at low energies.
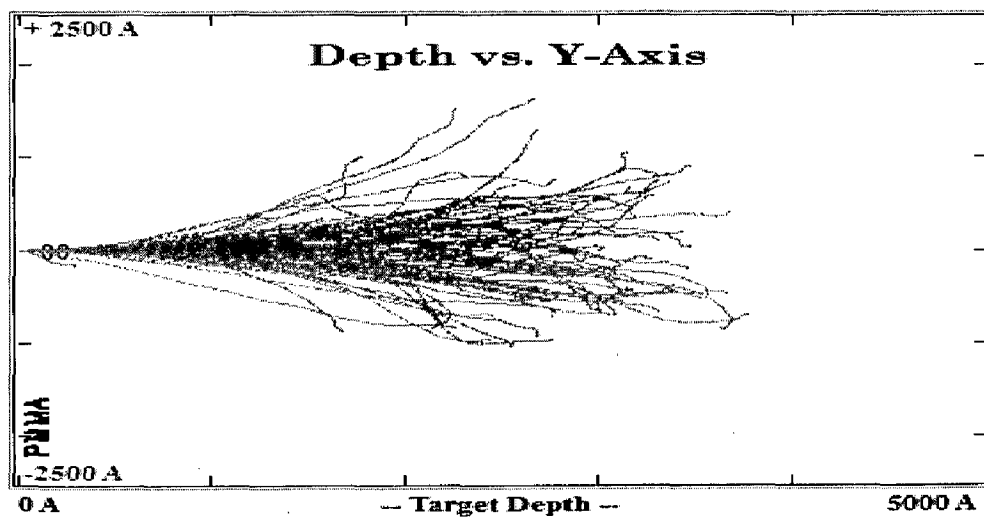
Fig. 4.1 Trajectory path of Oxygen ion of energy 63 keV in PMMA simulated by SRIM 2008

39

4.2.1 Absorbance

The absorption of electromagnetic radiation by polymeric materials in the ultraviolet and visible regions involves promotion of electronics in σ, π and n-orbitals from the ground state to higher energy states which described by molecular orbital. High charge state ion causes a high reactivity in an irradiated material and induces unique phenomena due to strong Coulomb potential [71]. It is expected that this high reactivity enhanced the productivity of damage in an irradiated materials compared to singly charge ion. The low energy HCIs are more effective to produced defect in surface or subsurface level [1].

The absorbance of the implanted samples decreased as the wavelength was increased from UV to the visible region (800 nm) and the absorbance was quite low in the NIR region (Fig. 4.2). The steady decrease in absorbance show the shift (decrease) in the band gap of irradiated PMMA could be due to formation of number of smaller units of PMMA due to chain (side) scission during ion implantation

An oscillating pattern of absorbance was observed in the range of 300 – 350 nm which could be due to hole transition that might take place due to formation of defects which produced due to HCIs [59]. The increase in absorption (decrease in band gap) might be due to conversion of PMMA (polymeric structure) into a hydrogen depleted carbon network due to the emission of hydrogen and other volatiles products which make it more conductive relatively [9,72]. This shift in the absorption may be produced in creation of free radicals or ions, which increases the energy of valence band and thus have a capability of polymers to conduct. This may be due to the higher rate of nuclear energy loss of incident ion, which affects the optical properties of polymers to a great extent [24].

40
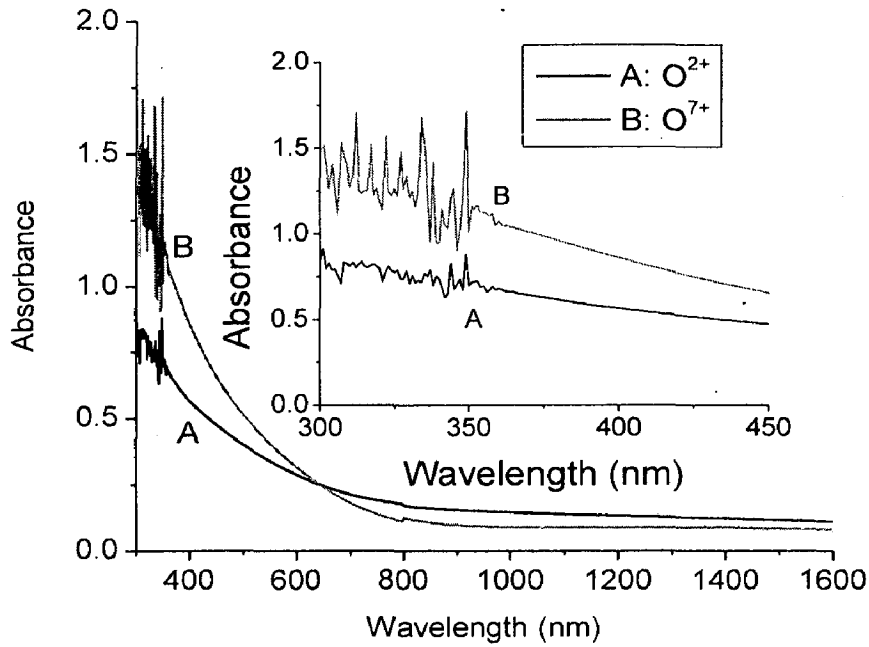
Fig. 4.2 Absorbance of Oxygen ion beam implanted PMMA with reference to pristine PMMA.

4.2.2 Transmittance

The optical transmission spectra of high charge state Oxygen ion of 63 keV implanted PMMA samples are presented in Fig. 4.3. There were two charge state ions O^{2+} and O^{7+} used. There is significant change in the optical transmission for the both the charge states. The lack of declination in case of 2+ ion beam implantation means that the polymer surface in this case is as hardly structurally modified as for the 7+ ion beam implantation at the same energy 63 keV. This could be due to the greater destruction occurs via a mechanism resulting in a significant change of the defect states density for lower but higher energy (> 50 keV) case, there may be some critical level of energy deposition into the surface layer is reached. This energy 50 keV reported as high energy for Si^+ ion implanted on PMMA [52]. HCI O^{7+} was show lower transmittance

compared to the lower charge state ion O^{2+} that might be due to high chare state produces higher defect density at same energy. This HCI O^{7+} show high transmittance in NIR region also due to defect density.
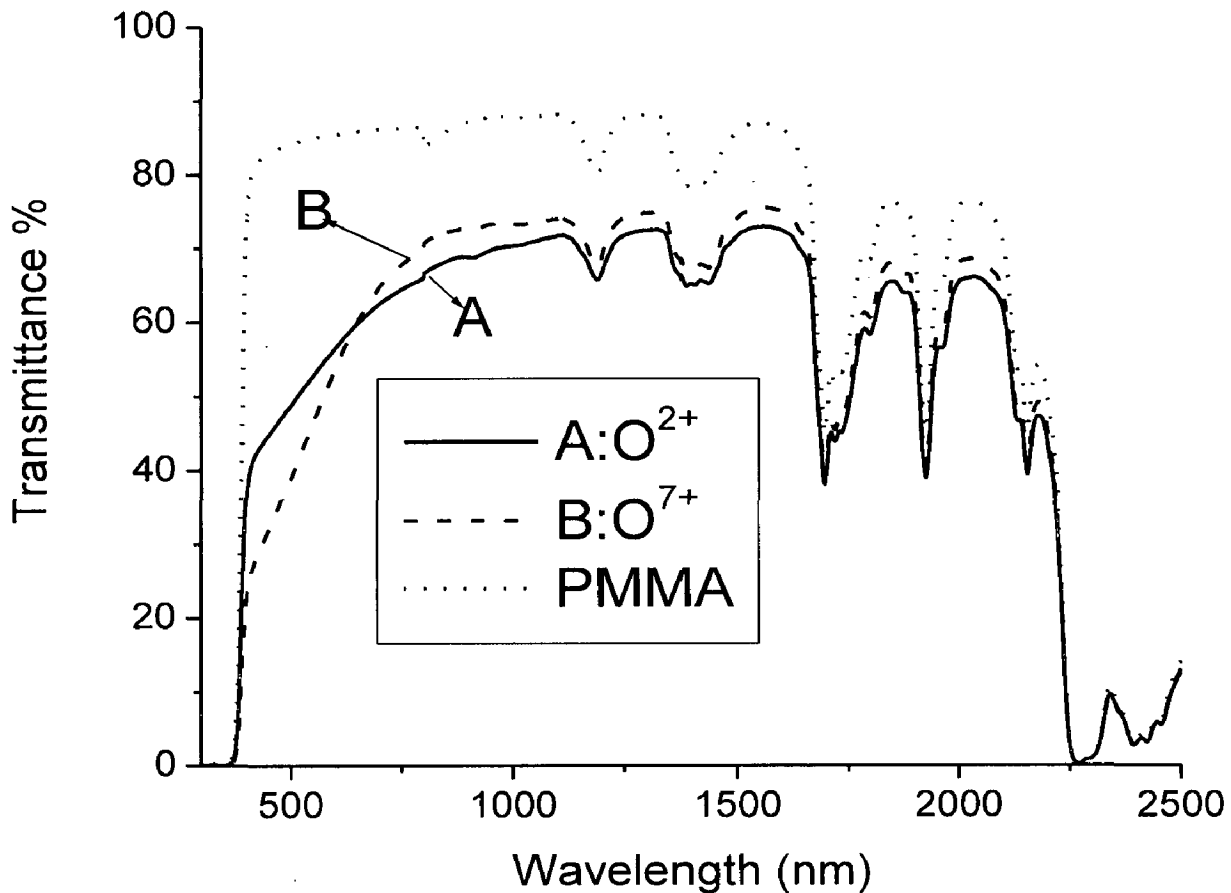
Fig. 4.3 Transmittance spectra of Oxygen ion beam implanted PMMA and pristine PMMA

4.2.3 Reflectance

The obtained in absorbance and transmittance results that O^{7+} effect higher as compared to O^{2+} were corroborated by recording the total reflectivity of implanted PMMA with respect to pristine PMMA. The implanted PMMA showed gradual increase in the total reflectivity with the increase

in wavelength of light from UV to visible region and the reflectivity in the NIR region was very high (~80-90%) as compared to the pristine PMMA (Fig. 4.4), where the O^{7+} ion beam implanted samples showed higher total reflectivity than O^{2+} implanted samples. But in the UV spectra the total reflectivity was higher for O^{2+} implanted samples. Further, a small rise in the reflectivity was observed for implanted samples at 305 and 350 nm which was also reported in Si^{+} ion implanted PMMA samples [19] and is attributed to the contribution of the reflection from the rear-side plane of the samples, may be from the layer of implanted atoms.
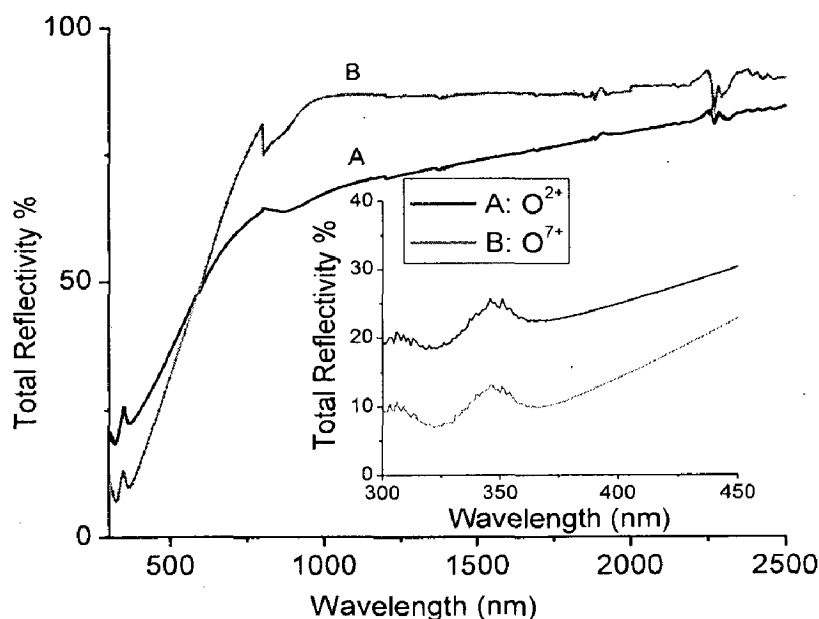
Fig. 4.4 Total reflectivity spectra of Oxygen ion beam implanted PMMA with reference to pristine PMMA.

4.2.4 Dielectric constant

It was calculated by equation as described in Chapter-3 and the obtained graph of dielectric constant vs. log frequency shown in Fig. 4.5. The pristine PMMA and irradiated PMMA had

show the usual dielectric constant as a dielectric material. The dielectric constant of both samples decreases with increase in frequency. By comparing the dielectric constants of ion implanted PMMA with pristine PMMA, two features were observed. First, irrespective of the charge states the dielectric constants of pristine PMMA and ion beam implanted PMMA were same ($\sim 10\pm2$) at higher applied frequencies (>20 kHz). Second, large dispersion in dielectric responses was noted and maxima at 800 Hz and 3000 Hz were observed at lower applied frequencies, which were due to natural resonance frequencies of electric dipole in PMMA.
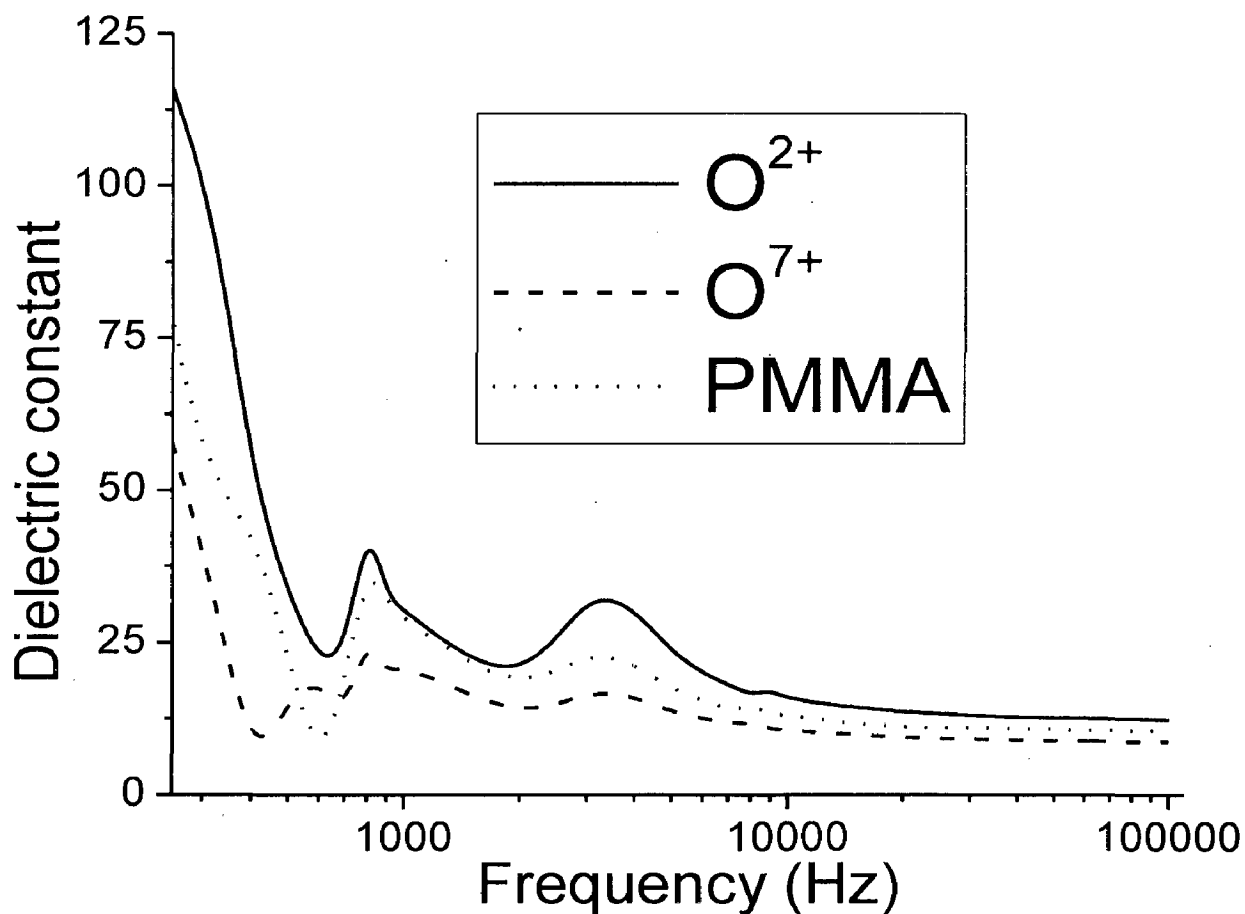
Fig. 4.5 Dielectric constant of O^{2+} & O^{7+} implanted PMMA samples and pristine PMMA

The observed increase in dielectric constant for O^{2+} implanted sample was attributed to more polarization of electric dipoles most likely at the interface of polymer and the layers of deposited O atoms during ion implantation. The dielectric constant observed at 3000 Hz for the O^{2+} implanted sample (34.63) was ~40% higher than the pristine sample (23.34). Implantation by O^{7+} did not show any differences from the pristine sample. Since the beam energy for both the charge states is same, so the increase in the measured dielectric constant may be thought to be due to the increase in the dose which was 10 folds higher for O^{2+}. It was found that O^{2+} was more effective to produced molecular polarizability as compared to O^{7+} ion beam which show the modification of PMMA with agreement absorption and other properties.

4.2.5 Dielectric loss

Fig. 4.6 shows strong frequency dependence of dielectric loss. It was almost constant for pristine and implanted PMMA above 1000 KHz. On comparing it of pristine and implanted PMMA three features were observed. First, each one was show its dielectric loss maxima which might be due to different charge and dose of ion beam used for implantation. Secondly, O^{2+} implanted dielectric loss maxima were broad and lower in magnitude at 600 Hz as compared to the pristine PMMA have dielectric it means it reduced the natural dielectric loss of PMMA. Thirdly, O^{7+} implanted PMMA was has dielectric maxima at 400 KHz where pristine PMMA minima exist which show the complete disappearance of natural PMMA dielectric loss. This might be due to the sharply fail in the induced charges or ions to followed the reversed field causing reduction in the electronic oscillations at particular frequency range.

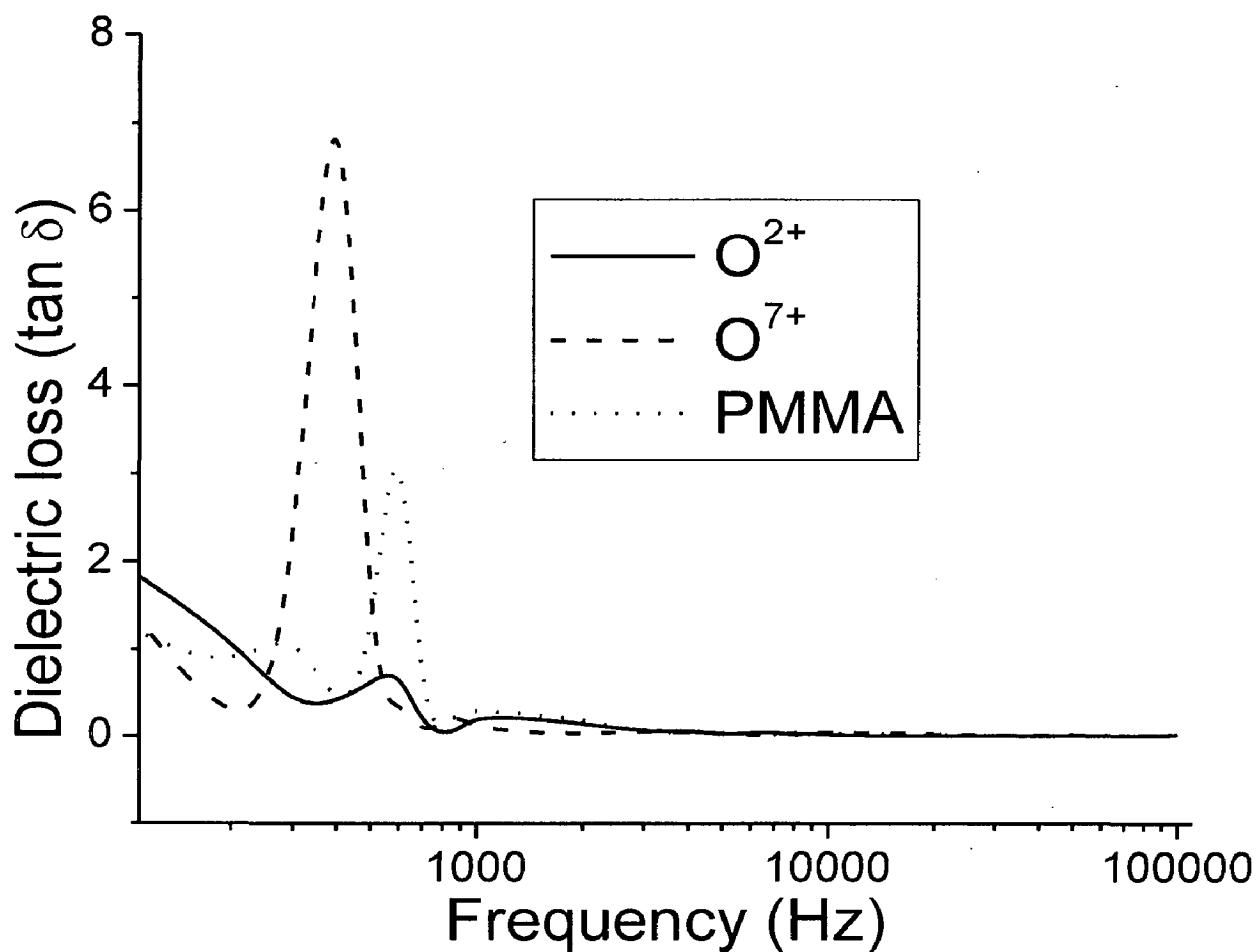Fig. 4.6 Dielectric losses of O^{2+} &O^{7+}implanted PMMA and pristine PMMA

4.2.6 Surface morphology

The surface morphology and dimensions of irradiated and pristine PMMA was recorded at 5 keV

in high vacuum 10^{-7} torr. The morphology of irradiated PMMA was recorded after measured the

dielectric constant. Silver paste thin film over the samples was removed by tissue paper dipped in

ethanol with simple hand. The etching of irradiated PMMA had been done by ultra-sonication in ethanol for 2-3 minutes.

The morphology and dimensions of surface tracks produced by 63 keV high charge state of Oxygen ions on PMMA change continuously. By comparing the FE-SEM structure of pristine and irradiated PMMA, some feature observed. Firstly, the look of irradiated PMMA samples were completely different from pristine which show the surface modification of PMMA as also recorded in optical and dielectric response. Secondly, ripples were observed in both cases, but in case of O^{2+} it was approximately double as compared to the O^{7+} implanted sample while O^{2+} dose was 10 times higher than O^{7+}, that might be responsible in change in it properties. The holes were present in both cases represent the defect tracks (Fig. 4.7b, 4.8f), the morphology of etched irradiated PMMA was different for O^{2+} & O^{7+} implantation.

The surface was changed as a shrunken plane and ripples due to heating resulted from oxygen ion bombarding. Due to high ion fluence, heavy irradiation damage took place.
Similar, surface-recovering and shrunken behavior of the oxygen ion irradiation-damaged plane was reported on surface of the PPC sample implanted with fluence of 10^{15} ions/cm^2 The ripples resulted from both heaviest irradiation damage and thermal shrinkage. The smoothening plane was formed due to surface-recovering. The surface-recovering occurred because of the maximum heating resulted from numerous oxygen ion bombarding. It is suggested that low energy oxygen ion implantation with lower fluence show less structural damage, and one with higher ion fluence resulted in heavier structural damage due to severer chain-scission.

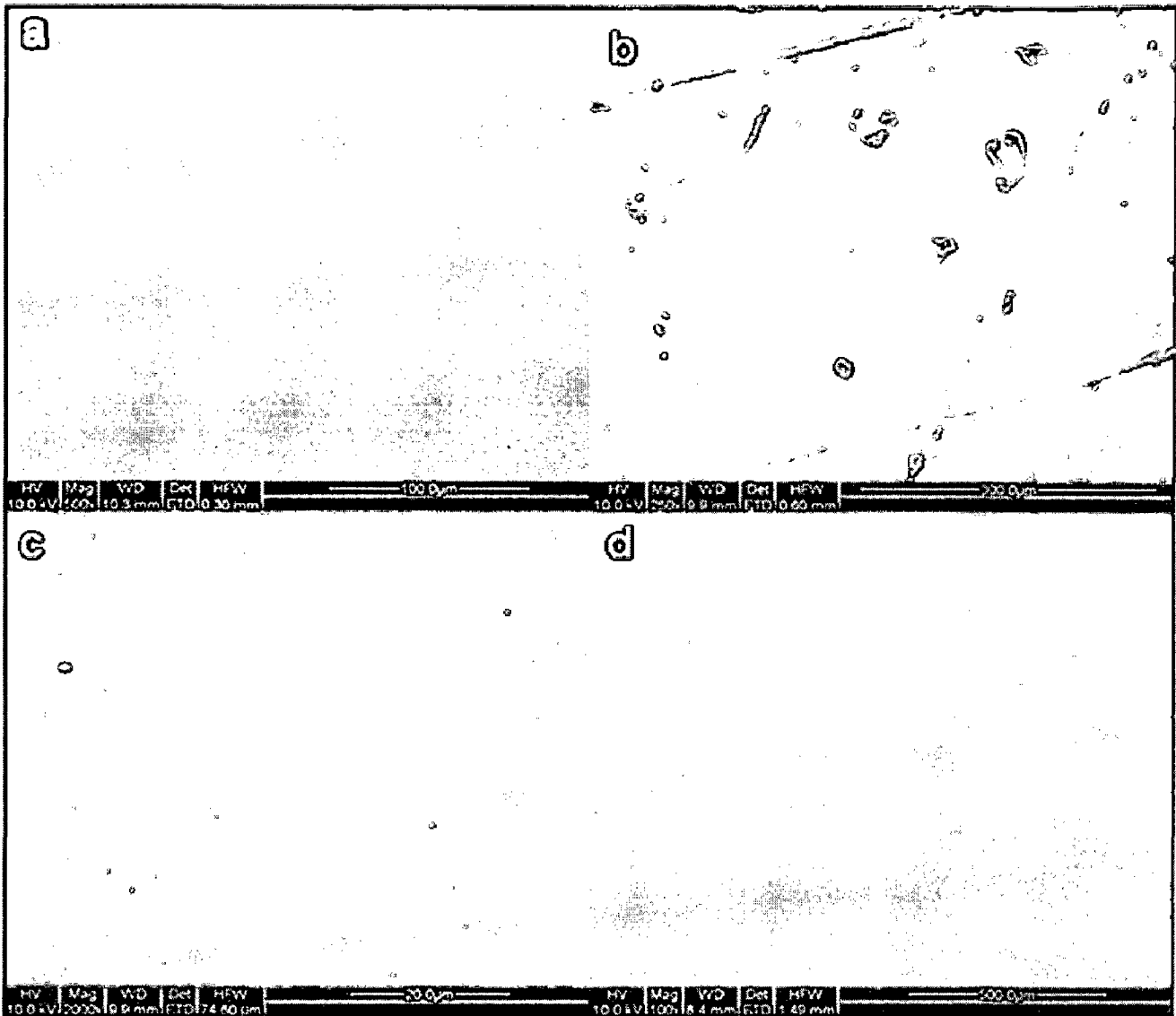Fig. 4.7 FE-SEM structures of (a) pristine PMMA, and (b, c) irradiated PMMA with O2+ ion beam of energy 63 keV of the fluence 1.4×10^{17} at different scale, (d) completely etched of irradiated PMMA.
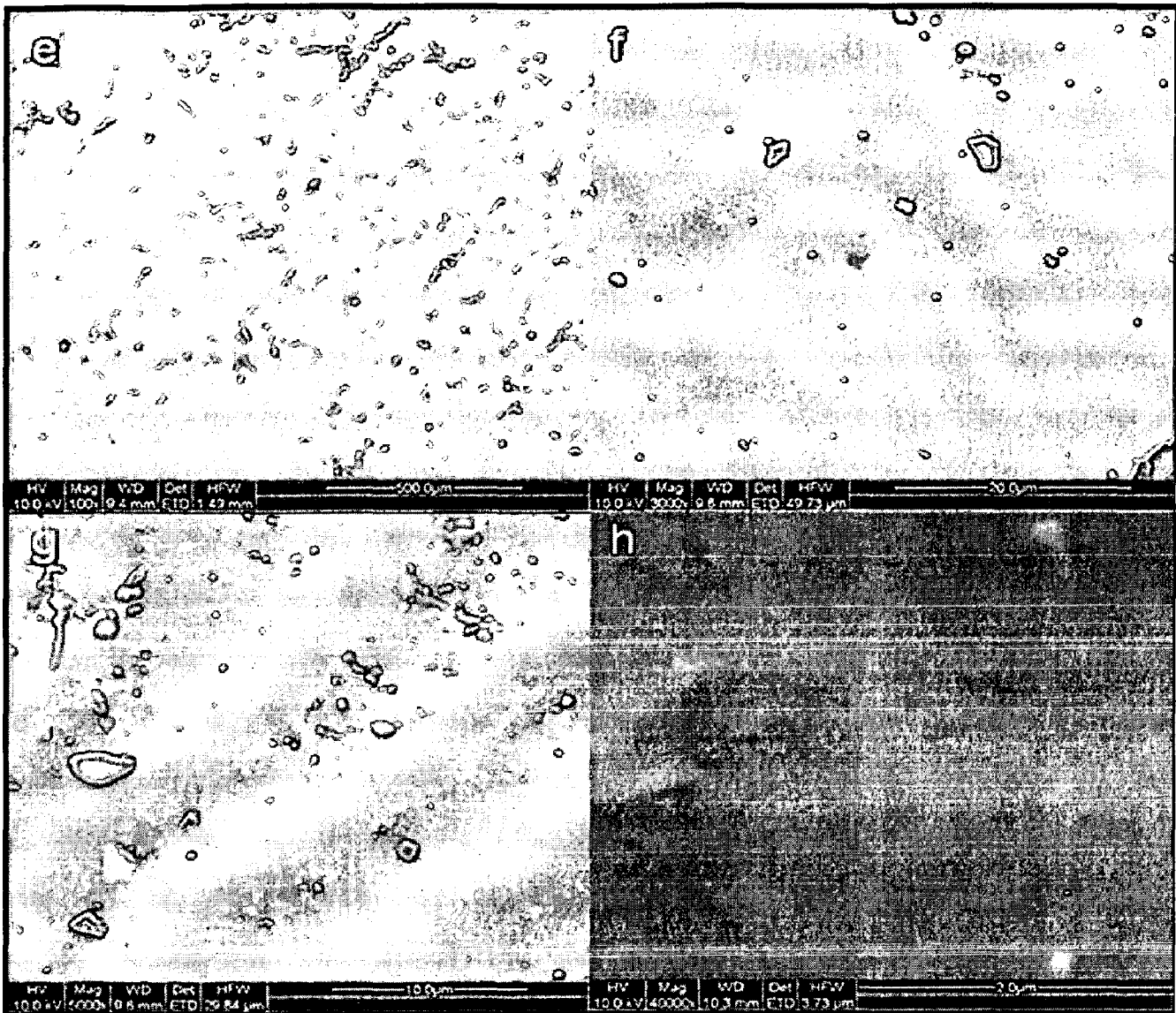
Fig. 4.8 FE-SEM structures of (e, f, g) irradiated PMMA with O^{7+} ion beam of energy 63 keV of the

fluence 10^{16} at different scale, (h) completely etched of O^{+7} ion irradiated PMMA.

CHAPTER 5

EFFECT OF N^{5+} AND O^{5+} ION BEAM IMPLANTATION ON PMMA

(POLYMETHYL METHACRYLATE)

5.1 Experimental

Commercially available PMMA (polymethyl methacrylate) sheet (Goodfellow, UK) of thickness

1 mm was also used to study effect of N^{5+} and O^{5+} ion beam effect on PMMA in present study.

The sample preparation section was same as discuss in Chepter-4. In this experimental scenario

two different ion beams, namely, N, O with high charge state (5+) were used. The energy of both

the ion beam was kept constant at 45 keV. The particle doses were varied, namely, 10^{14}, 10^{15},

10^{16} and 10^{17}. The beam current was $1 - 3.5$ μA. The absorbance spectra of implanted PMMA

samples were recorded over range 300-2500 nm. The pristine PMMA material was used for

reference material in order to eliminate the effect of unmodified PMMA contribution in

absorbance. The absorbance of all samples was measured under identical conditions at room

temperature. Diffuse reflectivity data for the N^{5+} and O^{5+} implanted PMMA samples were

obtained at near-normal incidence ($\sim 3°$) by Varian Carry 5000 UV–vis-NIR spectrophotometer.

The spectra were recorded over the wavelength range 300–2500 nm using the above instrument

equipped with external Praying Mantis diffuse reflectance accessory (integrating sphere). The

reference reflectance material used for the measurements was a Spectralon white standard—the

100% baseline was collected by SRS-99 (Labsphere Inc.). The diffuse reflectance of all samples

was measured under identical conditions at room temperature. In order to eliminate the

contribution of the sample holder (blackmat), its reflectance was accurately measured under the

same conditions in the spectrophotometer and it was subtracted from the spectra (auto zero base

line correction). The transmittance data was obtained at normal incidence in the wavelength

range 300-2500 nm. The dielectric responses of the implanted and pristine PMMA samples coated with thin film of silver paste were measured in capacitor mode (as chapter-2) at room temperature in the frequency range 300 Hz–0.1 MHz by LCR meter (Model 3532-50, HIOKI).

5.2 Results and discussion

The simulated distribution of 45 keV oxygen and nitrogen ion beam in PMMA and their mean ranges approximately 280 and 260 nm respectively obtained from SRIM 2008 calculation is
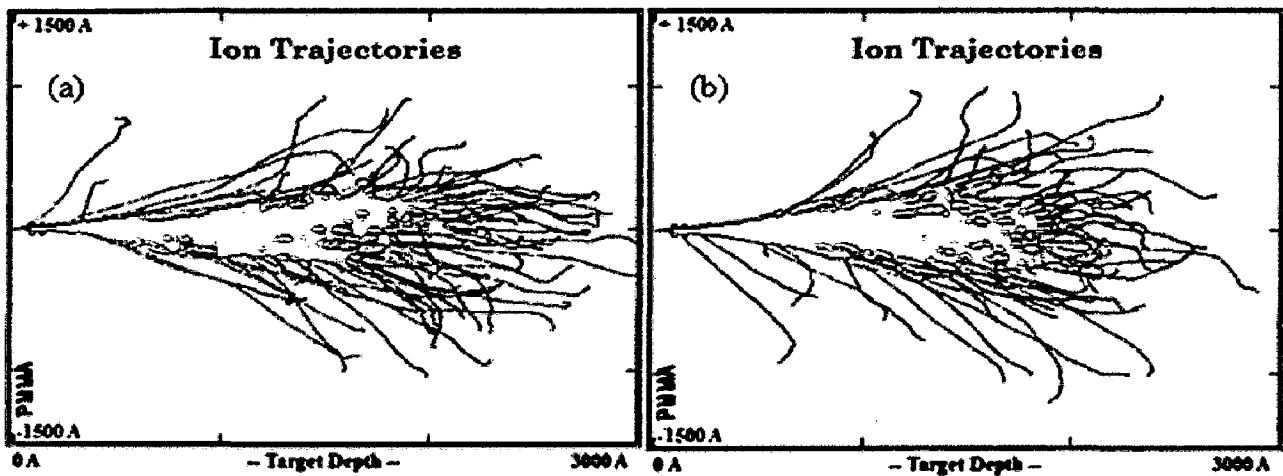
Fig. 5.1SRIM calculation for 45keV oxygen (a) and nitrogen (b) ion beam in PMMA
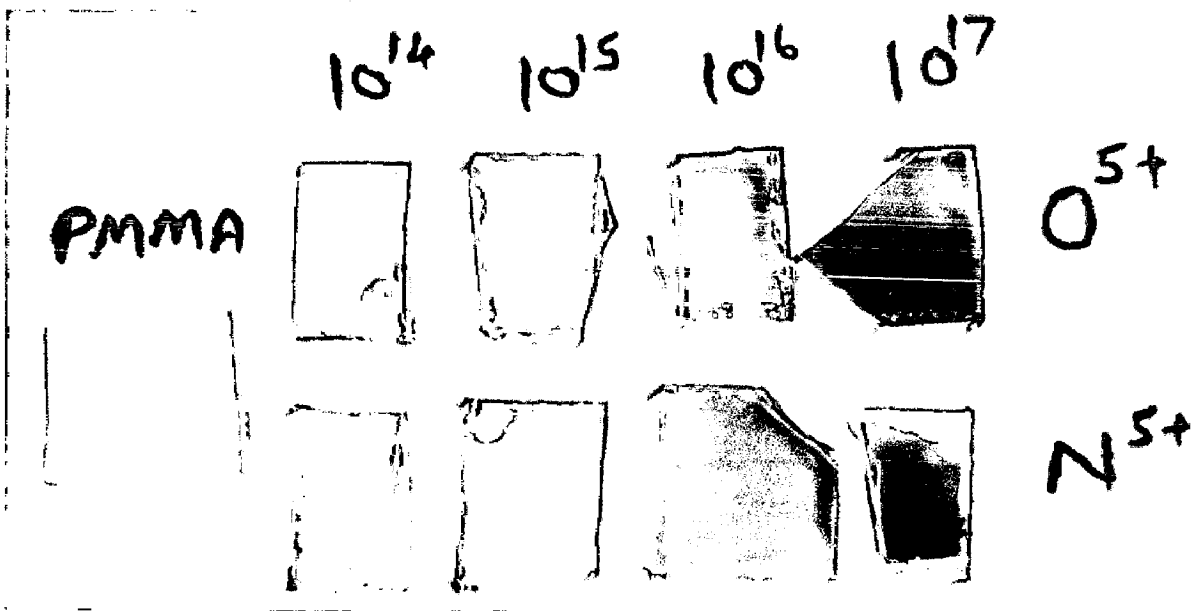
Fig. 5.2 photograph of pristine and O^{5+} and N^{5+} implanted PMMA.

51

given in fig. 5.1. The implanted samples physically appeared brown in colour (Fig.5. 2).

5.2.1 Absorbance

The absorption spectra of both the high charge state ion of N^{5+} and O^{5+} were similar in nature but change in intensity for different doses (Fig. 5.3, 5.4). The sharply decrease in absorbance in the
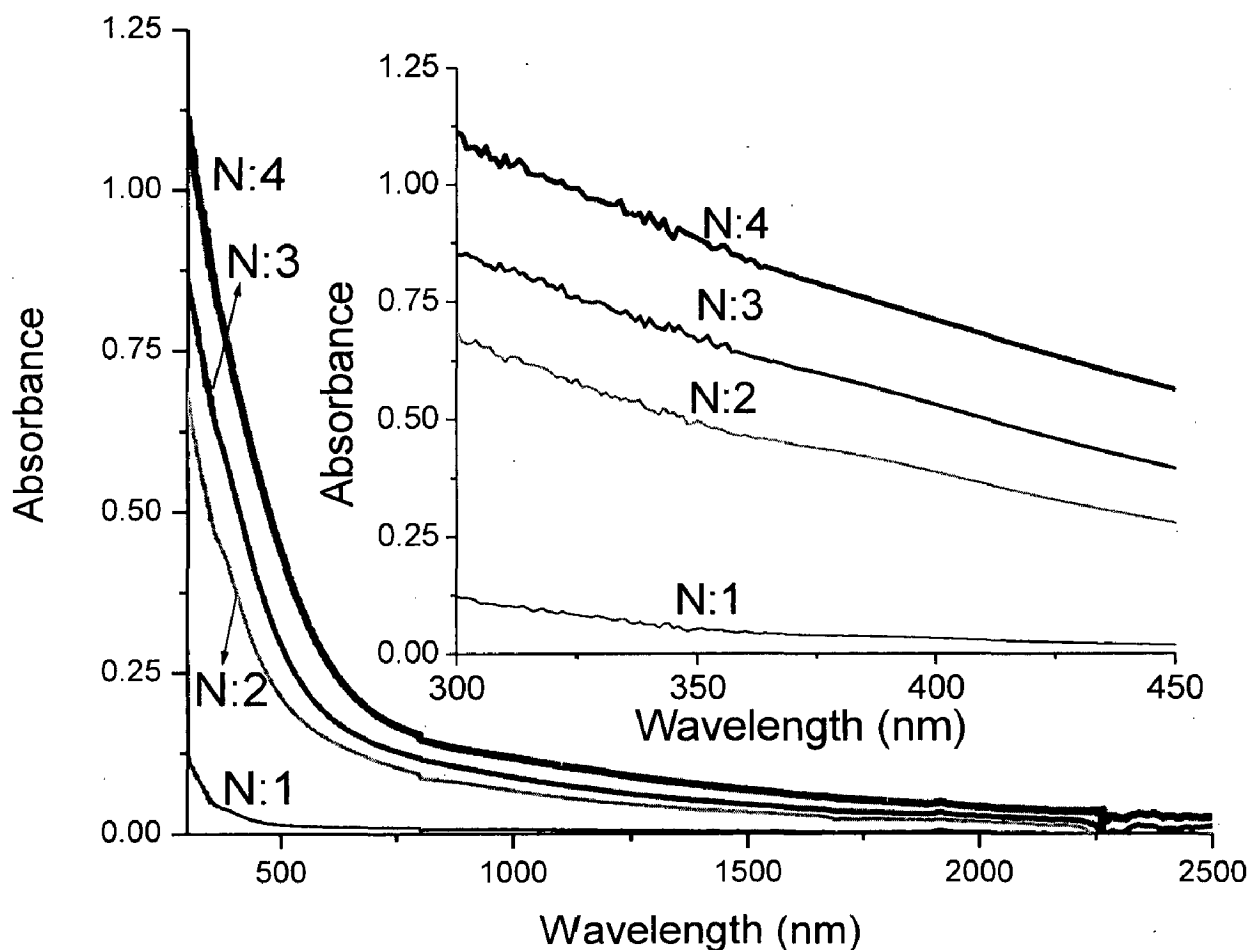
Fig. 5.3 UV-vis-NIR absorbance spectra of the material resulting from 45 keV N^{5+} ion implantation of PMMA samples. The doses are denoted as N:4(10^{17}); N:3(10^{16}); N:2(10^{15}); N:1(10^{14}); N:0(pristine PMMA).

UV- Vis region was due to the multiple scission of PMMA side chain because the bond energy

required to break are very small such as 3.65 eV for a C-C bond, 3.75 eV for a C-O bond and

4.28 eV for a C-H bond[73] in case of ion implantation. The oscillating pattern in the absorbance
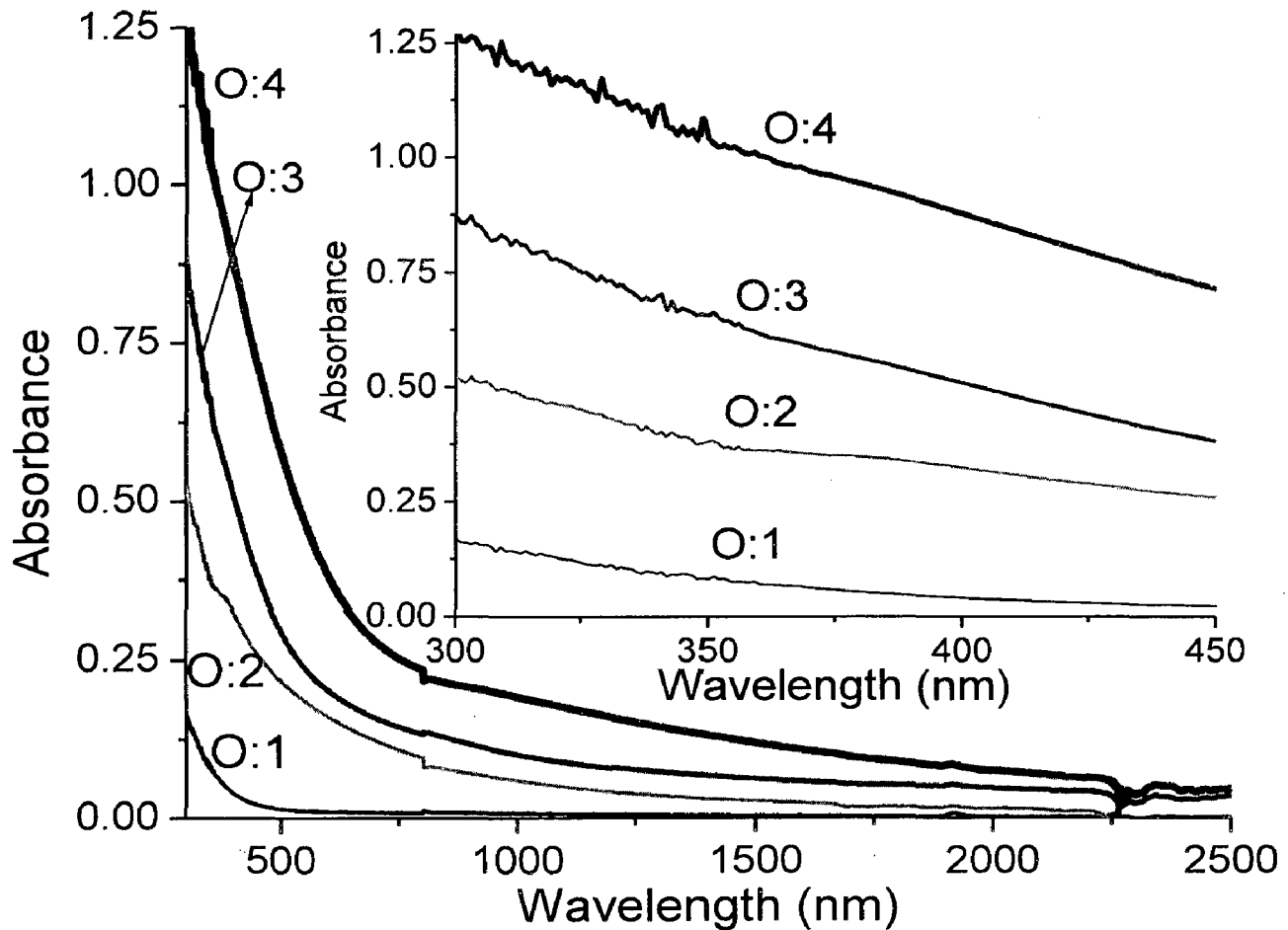
Fig. 5.4 UV-vis-NIR absorbance spectra of the material resulting from 45 keV O^{5+} ion implantation of PMMA samples. The doses are denoted as $O:4(10^{17})$; $O:3(10^{16})$; $O:2(10^{15})$; $O:1(10^{14})$; O:0(pristine PMMA).

was observed high for high doses in the range 300-350 nm which could be due to hole transition that might produced during defect formation. The decrease in band gap of implanted PMMA was due to the higher modification corresponding to increase in dose. The dose 10^{14} was not more effective for both the ion implantations. Whereas, in case of high ion dose modification higher that leads to the formation of conjugated double C=C bonds organized in a nano-clustered hydrogenated amorphous carbon material [74, 75].

Table 1 Dose dependence of absorbance of N^{5+} implanted PMMA samples at different wavelength

Dose, ions/cm^2	300 nm	700 nm	1100 nm	1500 nm	1900 nm
10^{14}	0.12329	0.00963	0.00566	0.00334	0.00307
10^{15}	0.68709	0.11441	0.05589	0.03236	0.02002
10^{16}	0.85103	0.1403	0.07552	0.04459	0.02992
10^{17}	1.11135	0.1876	0.10496	0.06687	0.04562

Table 2 Dose dependence of absorbance of O^{5+} implanted PMMA samples at different wavelength

Dose, ions/cm^2	300 nm	700 nm	1100 nm	1500 nm	1900 nm
10^{14}	0.16803	0.00904	0.00671	0.00385	0.00412
10^{15}	0.52327	0.12228	0.04942	0.02677	0.01725
10^{16}	0.87414	0.15818	0.08802	0.06217	0.0512
10^{17}	1.28238	0.27812	0.17536	0.11902	0.08347

The modification observed in UV-Vis region was high for O^{5+} and N^{5+} ion beam case (Table 1, 2). It was observed that O^{5+} implanted PMMA have higher absorbance as compared to N^{5+} implanted PMMA in UV-Vis region for approximately each dose and O^{5+} have 10% higher absorbance with respect to N^{5+} implanted PMMA at 300 nm and 10^{17} dose (Fig. 5.5).

Therefore, O^{5+} was more effective for modification as compared to N^{5+} that could be due to higher chemical structure modification in case of O^{5+} ion implantation, which was also reported in Oxygen and Nitrogen RF plasma treated PMMA [6]. The modification was observed maximum at 300 nm (shortest wavelength) for dose 10^{17} (maximum dose used in present experiment) maximum in UV region for both cases where O^{5+} was prominent.
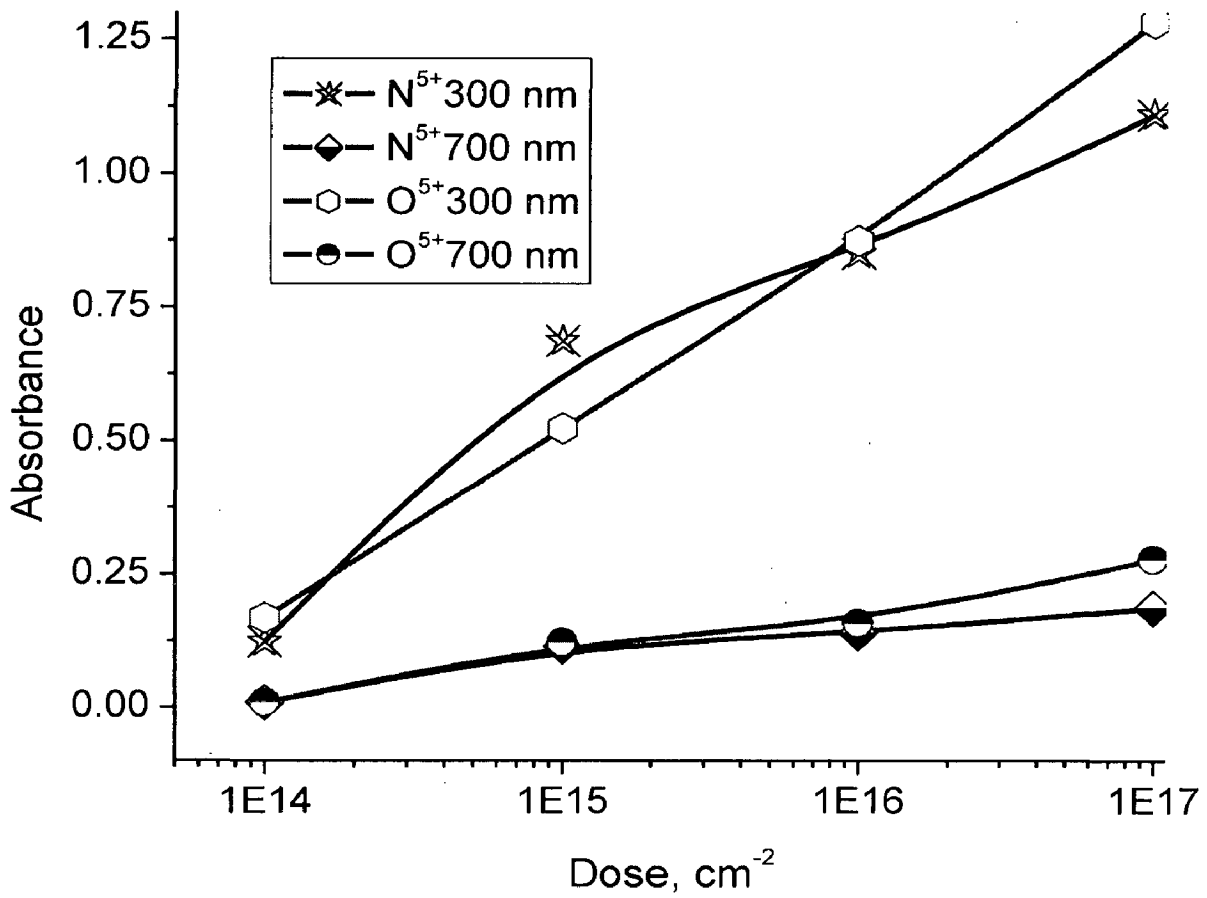
Fig. 5.5 Dose dependence of absorbance enhancement measured at wavelength 300 nm and 700 nm for N^{5+} & O^{5+} ion implanted PMMA samples.

5.2.2 Transmittance

The transmittance in the near UV and in visible region was decreases as the ion dose increases

for both the cases and found to be O^{5+} more prominent in case of 10^{17} dose, which was due to
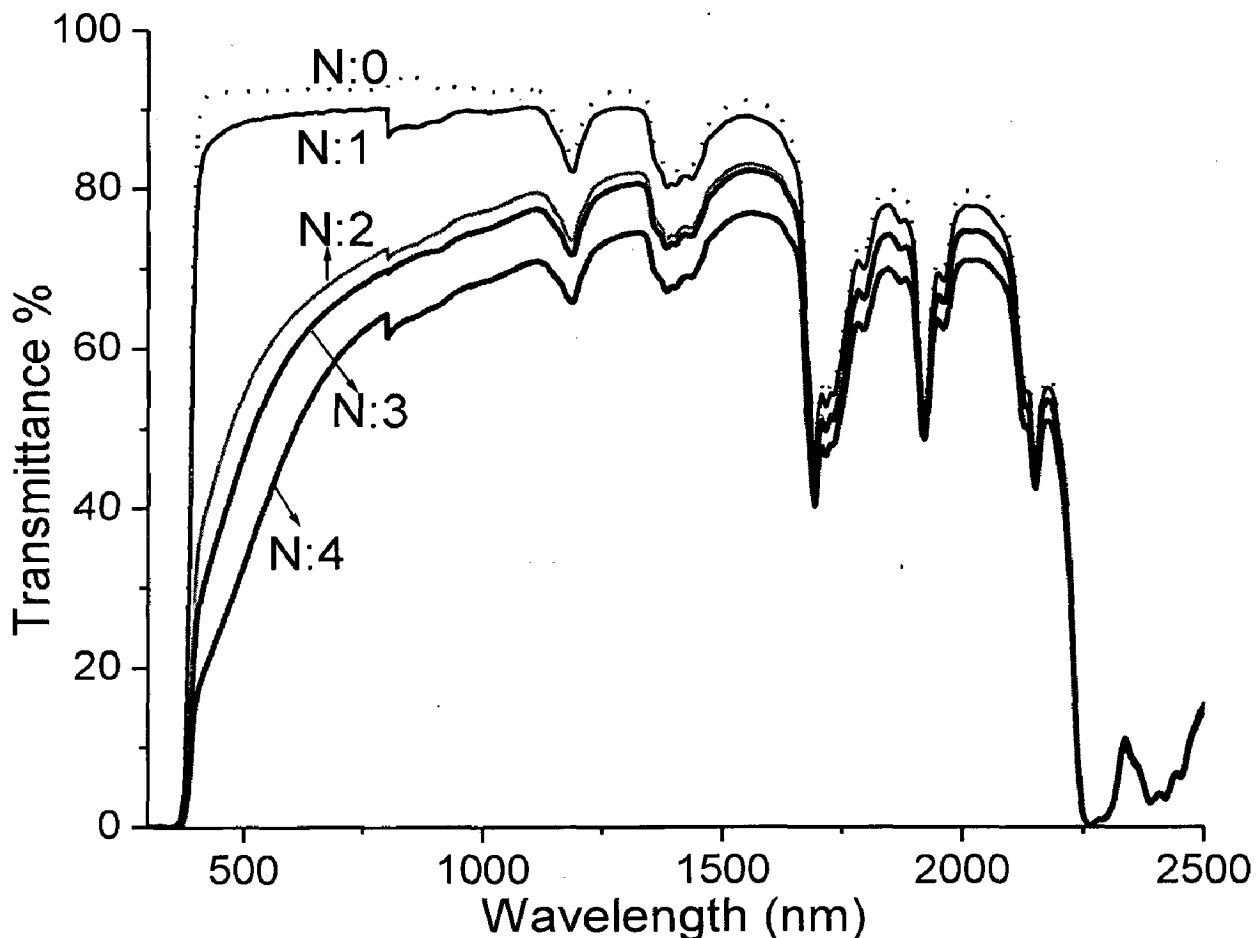
Fig. 5.6 UV-vis-NIR transmittance spectra of the material resulting from 45 keV N^{5+} ion implantation of PMMA samples. The doses are denoted as Fig. 5.3.

formation of smaller (multiple size) of PMMA due to the chain scission during ion implantation. At higher implantation dose, the effect of the ion implantation on the transmittance cannot be readily tracked. As reported that an aggregation of the C- rich clusters through unsaturated

interconnections takes place in high dose implantation regime [71]. In the higher wavelength range, the PMMA changes after ion implantation were less pronounced specialy after 1600 nm.

Fig. 5.7 UV-vis-NIR transmittance spectra of the material resulting from 45 keV O^{5+} ion implantation of PMMA samples. The doses are denoted as Fig. 5.4
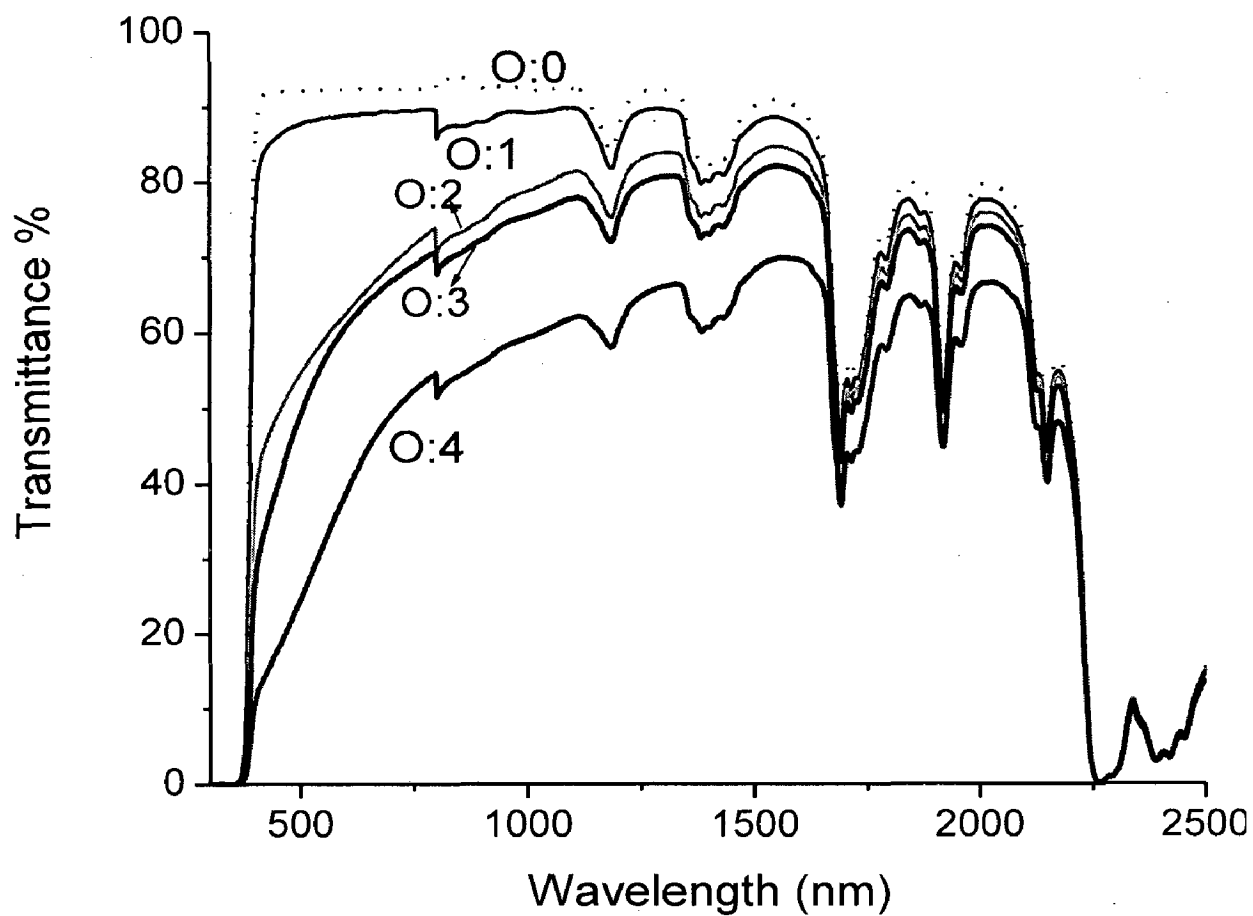
5.2.3 Diffused reflectance

In order to see the contribution in diffuse reflectivity (DR), N^{5+} and O^{5+} ion was implanted on PMMA. It was observed that O^{5+} and N^{5+} implanted PMMA have very high DR as compared to reported in literature for Si^+ implanted PMMA, while pristine PMMA have same DR [19, 20] which might be due to high charge state ion of energy 45 keV. For both the ion implantation of dose 10^{15}, DR of implanted PMMA samples was increases with wavelength in 380-800 nm range as also reported in literature [19, 20]. As an expectation well pronounced minima range observed in the wavelength range 350-380 nm for 10^{15} dose O^{5+} and N^{5+} implanted PMMA which could be due to short range interference effect [74] of multiple scattering and reflection of waves which takes place during diffusion of light, such minima peak was also observed in Si^+ implanted PMMA of dose 10^{17} at~500 nm [19].

As an exception, DR of PMMA samples implanted at dose 10^{17} exhibits wave like pattern in wavelength range 350-800 nm for O^{5+} & N^{5+} ions which decreases with increase in wave length in N^{5+} implanted PMMA sample and almost constat in O^{5+} implanted PMMA sample, that could be due to higher modification through high charge state ion leads to decrease in number of subsurface interface [19].

DR of the O^{5+} and N^{5+} implanted PMMA samples were constant 10^{15} at dose and increases with wavelength at dose 10^{17} in UV range 300-350 nm. The O^{5+} implanted samples were show two times higher DR as compared to N^{5+} implanted PMMA samples for both dose (Fig. 5.8, 5.9), which is due higher chemical modification through O^{5+} ion and higher topological modification through N^{5+} that leads to short range interference [19] as also reported for single charge state ion of oxygen and nitrogen on PMMA [6].

The DR spectra are the result of the coupling of both optical absorption and interference formed by multiple reflection and scattering of directionally and diffuse transmitted light. The transmittance observed very weak due to absorption and reflection, the secondary reflection from the back side of the high dose implanted PMMA samples diminishes and is fully eliminated, thereby the DR of these samples results due the formation of number of subsurface during ion implantation.

Fig. 5.8 Diffuse reflectance spectra recorded for of O^{5+} implanted on PMMA samples with energy 45 KeV in wavelength range 300-2500 nm.

The DR of O^{5+} and N^{5+} implanted PMMA samples were increases with wavelength as well as with dose in the range 800-2500 nm which is due to the reflectance from the modified and unmodified interface because transmitted intensity very high in this region as in Fig. 5.8, 5.9. The changes in DR are due to modification of polymer surface and subsurface region upon ion implantation
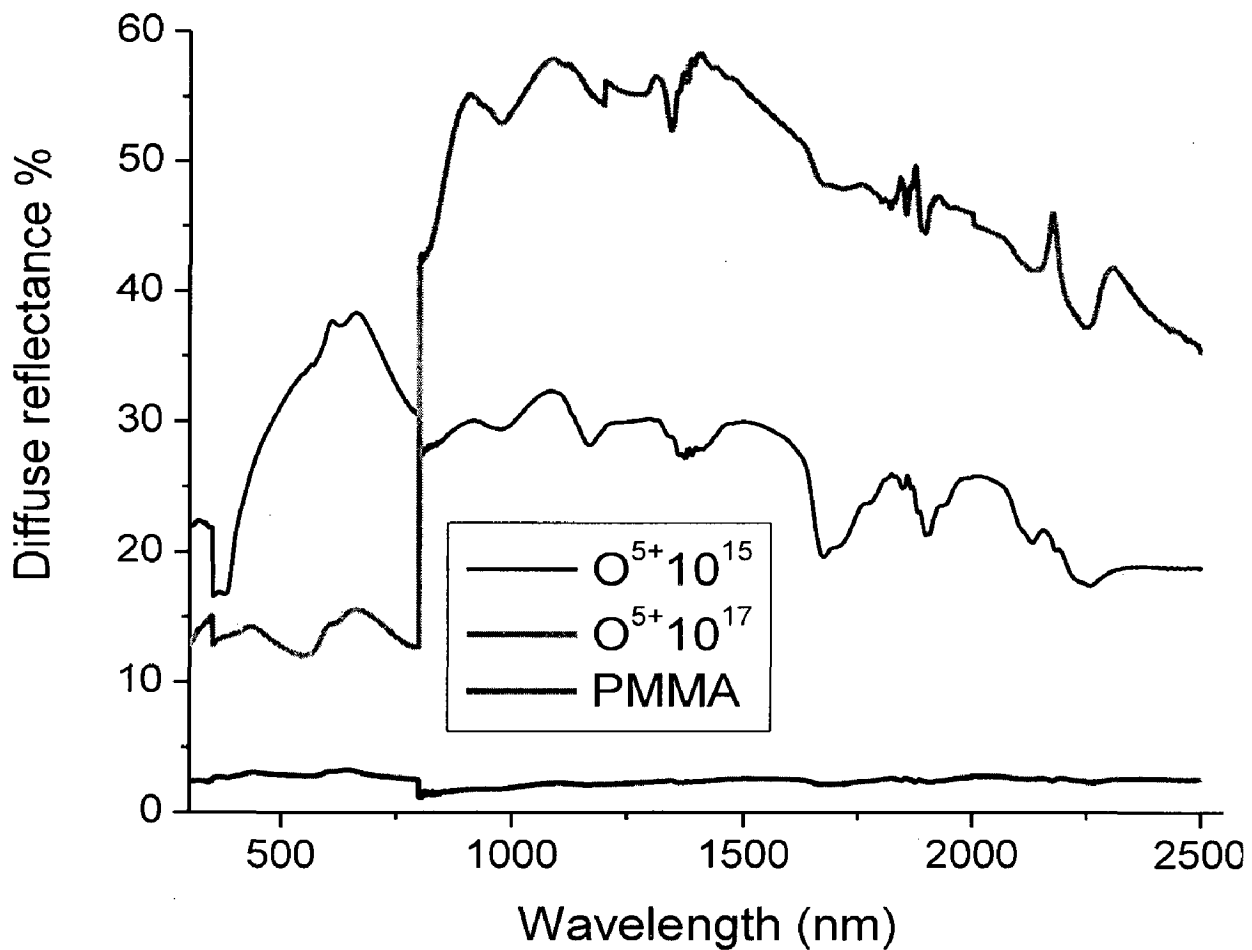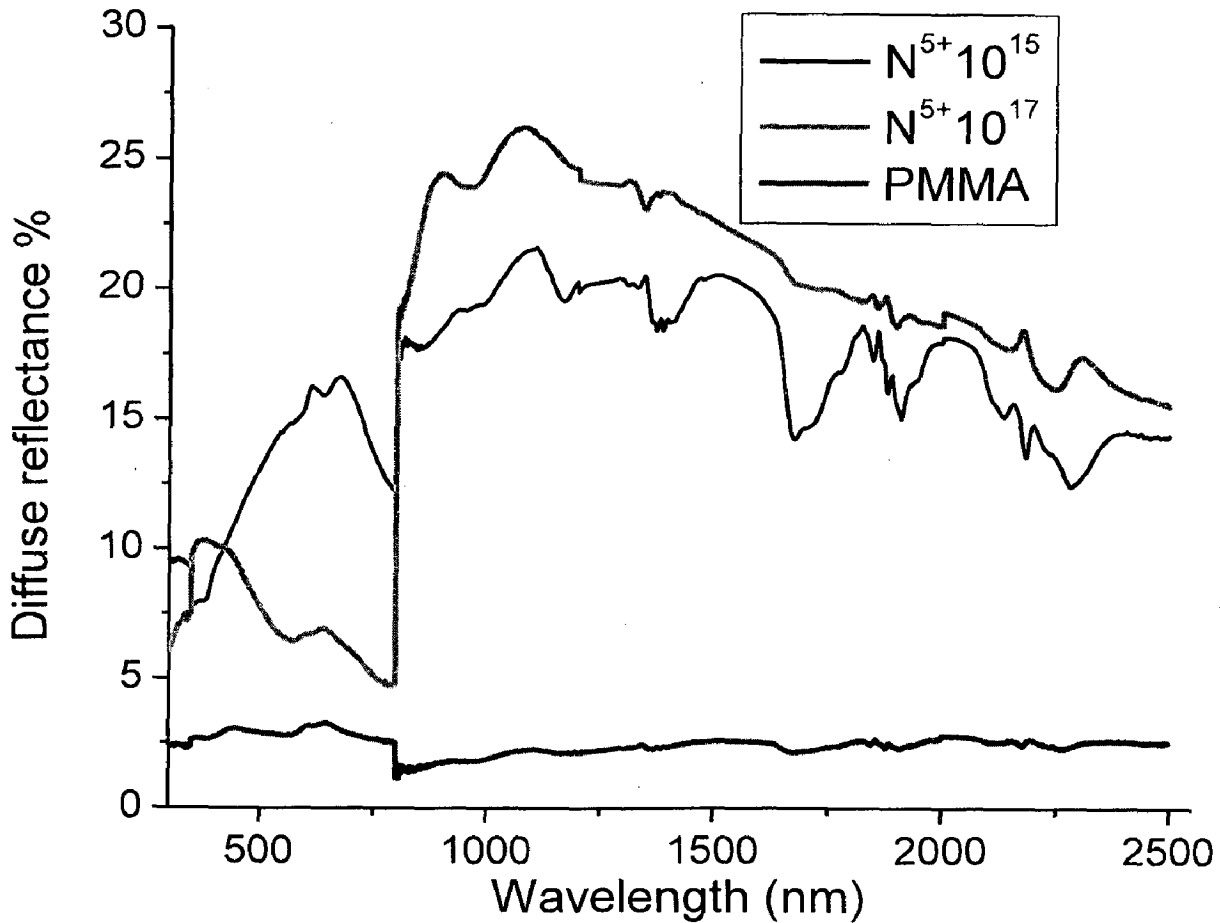

Fig. 5.9 Diffuse reflectance spectra recorded for of N^{5+} implanted on PMMA samples with energy 45 KeV in wavelength range 300-2500 nm.

The DR were increases with wavelength and dose for higher wavelength (>800 nm) while in case of smaller wavelength (<800 nm) increases with wavelength for 10^{15} dose and decreases for 10^{17} dose.
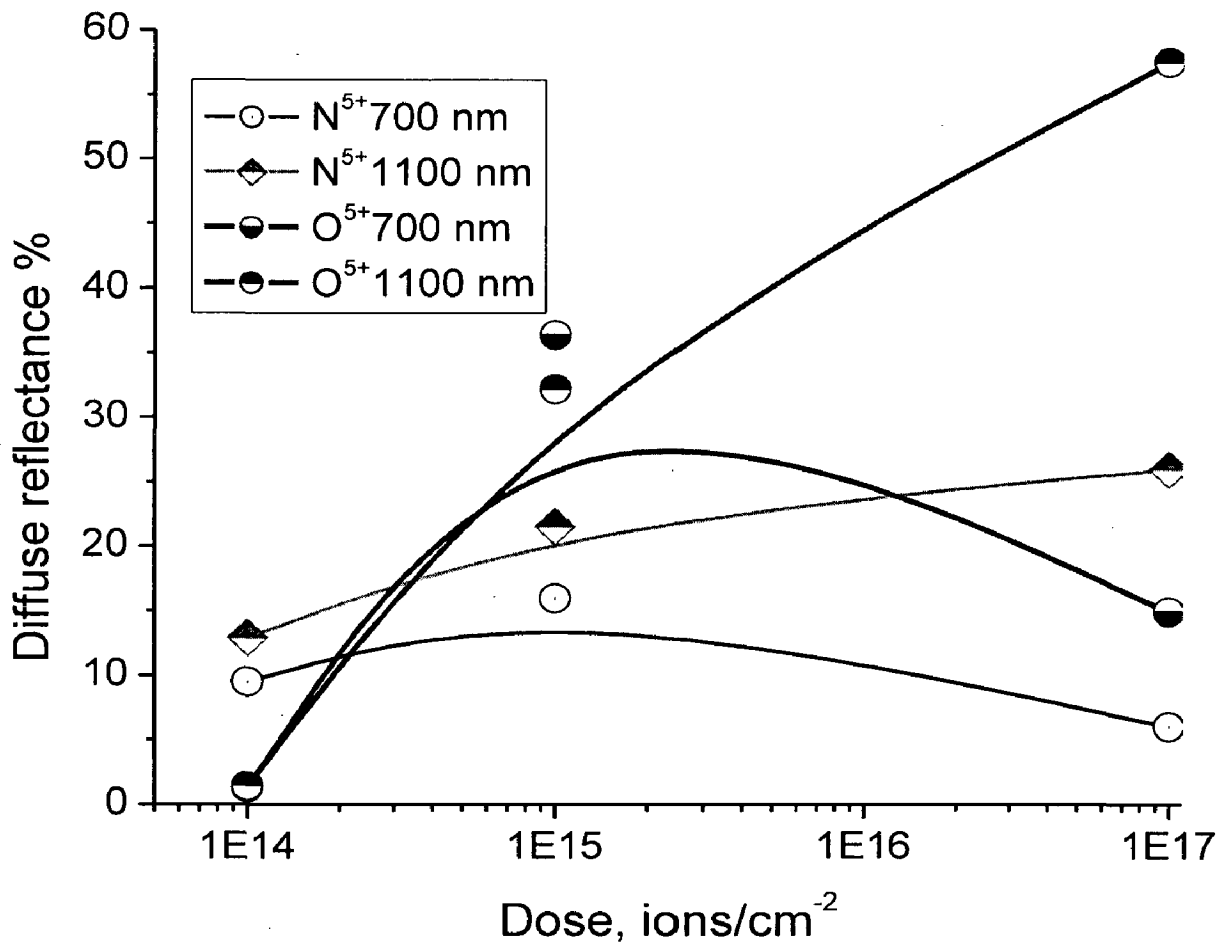
Fig. 5.10 Diffuse reflectance spectra recorded for of O^{5+} implanted on PMMA samples and N^{5+} implanted on PMMA samples with energy 45 KeV at various doses at maximum effective wavelength of visible region 700 nm and 1100 nm of NIR.

This behavior can be attributed to a combined effect from- (1) the increase of the refraction index of the buried ion implanted layer with the increasing ion implantation dose [75] and change in surface and number of subsurface layer; and (2) ion modified surface roughness.

The PMMA was more sensitive for O^{5+} ion as compared to the N^{5+} ion implantation (Fig. 5.10).

It is characterized by higher concentration of conjugated double C=C bonds created by C-H bond degradation upon ion implantation. Therefore, the comparison of DR of both O5+ and N^{5+} ion implanted PMMA materials sample and measured under identical experimental conditions, suggests that the formed ion implanted layer, the corresponding buried diffusive interface, distribution of ion & charge and number of interfaces within PMMA, are involved in the DR mechanism.

CHAPTER 6

Conclusion

The enhancement in absorption, reflectivity, transmittance and surface morphology were closely related to the charge state ion of oxygen and nitrogen as well as on the ion fluences. Low energy and high charge state ions modified the PMMA surface due to chain scission. In addition, it could lead to surface modification by formation of voids and holes inside the surface which was evidenced from hole transition, observed in UV-vis spectra. The diffuse reflectivity of O^{5+} ion of energy 45 keV irradiated PMMA have two times than N^{5+} ion of same energy irradiated PMMA. The DR of O^{5+} and N^{5+} implanted PMMA increases with ion fluence in NIR and UV region while in visible region reverse of this. Thus, O^{5+} is more effective for modification as compared to N^{5+} ion. The absorbance of O^{5+} and N^{5+} implanted samples were increase with ion fluence in all regions.

The surface modification with low energy and high charge state ion was achieved to be higher as compared low charge state ions. O^{7+} implanted PMMA results in lower dielectric constant as compared to the pristine while O^{2+} shows little higher. This might indicate the tenability of molecular polarization of dipoles in PMMA and O^{2+} implanted PMMA. The shrunken and ripples observed on the O^{2+} implanted PMMA had two times larger wavelength as compared to the O^{7+} implanted PMMA, which was due to higher potential energy of O^{7+} ion.

The irradiation with low energy and high charge state ion beam of oxygen and nitrogen were successfully used for modifying surface of PMMA.

REFERENCES

[1] J. D. Gillaspy, J. Phys. B: At. Mol. Opt. Phys. 34, R93 (2001).

[2] J. R. Rasmussen, E. R. Stedronsky, G. M. Whitesides, J. Am.Chem. Soc., 99(14), 4736 (1977).

[3] R. G. Nuzzo, G. Smolinsky, Macromolecules 17, 1013 (1984).

[4] U. Schulz, P. Munzert, N. Kaiser, Surf. Coat. Tech., 142-144, 507 (2001).

[5] J. Lai, B. Sunderland, J. Xue, S. Yan, W. Zhao, M. Folkard, B.D. Michael, Y. Wang, Appl. Surf. Sci., 252(10), 3375 (2006).

[6] D. Dorranian, Z. Abedini, A. Hojabri, M. Ghoranneviss, Journal of Non-Oxide Glasses, 1, 217 (2009).

[7] D W Thomas, C Foulkes-Williams, P T Rumsby, M C Gower, Laser Ablation of Electronic Materials (1992).

[8] S. X. Liu, J. T. Kim, S. Kim, Journal of Food Science, 73, 143 (2008).

[9] A. Bauer, J. Ganz, K. Hesse, E. KBhler, Applied Surface Science, 46, 113 (1990).

[10] D. Atias, K. A. Rabeah, S. Herrmann, J. Frenkel, D. Tavor, S. Cosnierd, R. S. Marks, Biosensors and Bioelectronics 24, 3683 (2009).

[11] Z. K. Wang, H. Y. Zheng, C. P. Lim, Y. C. Lam, SIMTech technical reports, 11, 23 (2010).

[12] R. Nathawat, A. Kumar, N.K. Acharya, Y.K. Vijay, Surf. Coat. Tech., 203(17-18), 2600 (2009).

[13] A. Kondyurin, P. Naseri, K. Fisher, D. R. McKenzie, M. M.M. Bilek, Polymer Degradation and Stability, 94, 638 (2009).

[14] W. R. Zeng, S. F. Li, W. K. Chow, Journal Of Fire Science, 20(4), 297 (2002).

[15] M. Ozdemir, C. U. Yurteri, H. Sadikoglu , Crit. Rev. Food Sci. Nutr. 39, 457 (1999).

[16] L. E. Nita, A. Ioanid, C. M. Popescu, I. Neamtu, G. E. Ioanid, A. P. Chiriac, Rom. Journ. Phys. 50, 755 (2005).

[17] E. H. Lee, Nucl. Instrum. & Meth. B 151, 29 (1999).

[18] Y. Koval, T. Borzenko, S. Dubonos, J. Vac. Sci. Technol. B 21 (2003)

[19] G. B. Hadjichristov, 1. L. Stefanov, B. 1. Florian, G. D. Blaskova, V. G. Ivanov, E. Faulques, Appl. Surf. Sci., 256, 779 (2009)

[20] S. Balabanov, T. Tsvetkova, E. Borisova, L. Avramov, L. Bischoff, J. Zuk, Journal of Physics: Conference Series 223, 012032 (2010) .

[21] E. K. Her, H. S. Chung, M. W. Moon, K. H. Oh, Nanotechnology, 20, 285301 (2009).

[22] S. Seki, S. Tsukuda, K. Maeda, Y. Matsui, A. Saeki, S. Tagawa, Physical Rev., B 70, 144203 (2004).

[23] S. Wolff, B. Lägel, S. Trellenkamp., Microelectronic Engineering, 87, 1444 (2010).

[24] R. K. Dutta, J. A. Van Kan, A. A. Bettiol, F. Watt, Nucl. Instr. Meth. B 260, 464 (2007).

[25] A. Saha, V. Chakraborty, R. K. Dutta, S. N. Chintalopudi, Rad. Phys. & Chem., 62, 429 (2001).

[26] A. A. Bettiol, K. Ansari, T. C. Sum , J. A. van Kan, F. Watt, Proceedings of SPIE, 5347, 255 (2004)

[27] R.C. Ramola, S. Chandra, A. Negi, J. M. S. Rana, S. Annapoorni, R. G. Sonkawade, P. K. Kulriya, A. Srivastava, Physica, B 404, 26 (2009).

[28] R. C. Ramola, S. Chandra, J. M. S. Rana, R. G. Sonkawade, P. K. Kulriya, F. Singh, D. K. Avasthi, S. Annapoorni, J. Phys. D: Appl. Phys. 41, 115411 (2008).

[29] A. M. P. Hussain, D. Saikia, F. Singh, D. K. Avasthi, A. Kumar, Nucl. Instr. and Meth. in phys. Res., B 240, 834 (2005) .

[30] A. Negi, A. Semwal, S. Chandra, R. V. Hariwal, R. G. Sonkawade, D. Kanjilal, J. M. S. Rana, R. C. Ramola, Radiation Measurements, 46, 127 (2011).

[31] K. Ichiki, S. Ninomiya, Y. Nakata, Y. Honda, T. Seki, T. Aoki, J. Matsuo, Appi. Sur. Sci., 255, 1148 (2008)

[32]J. S. Fletcher, J. C. Vickerman, Anal. Bioanal. Chem., 396, 85 (2010)

[33] T. Mouhib, A. Delcorte, C. Poleunis and P. Bertrand. Surf. Interface Anal., 43, 175 (2011).

[34] S. Youmeri, Z. Zhiyong, W. Zhiguang, J. Yunfan, L. Jie, H. Mingdong, Z. Qinxiang, Nucl. Inst. and Meth. Phy. Res. B 209, 188 (2003).

[35] Y. Hama, K. Hamanaka, H. Matsumoto, T. Takano, H. Kudoh, M. Sugimoto, T. Seguchi, Radiat. Phys. Chem. 48 (5), 549 (1996).

[36] Seguchi T, Kudoh H, Sugimoto M, Hama Y, Nucl. Inst. and Meth. B 151, 154 (1999).

[37] Mehta G K Nuclear Inst. and Meth. in Phy. Res. A 382, 335 (1996)

[38] S. Bolhuis et al. / Nuclear Instruments and Methods in Physics Research B 267, 2302 (2009)

[39] S. Bouffard, B. Gervais, C. Leroy, Nucl. Instr. Meth., B 105, 1 (1995).

[40] A. Chapiro, Nucl. Instr. Meth. B 105, 5 (1995).

[41] M. Komuro, N. Atoda, H. Kawakatsu, J. Electrochem. Soc., 126(3), 483 (1979).

[42] T. M. Hall, A. Wagner And Lp. Thompson, I. Appl. Phys. 53, 3997 (1982).

[43] P. F. Conforti, M. Prasad, B. J. Garrison, Acc. Chem. Res. 41(8), 915 (2008)

[44] Singh, S., Prasher, S., Nucl. Instrum. Methods B 244, 252 (2006).

[45] P. Singh, R. Kumar, H. S. Virk, R. Prasad, Indian Journal of Pure & Applied Physics, 48, 321 (2010).

[46] Seguchi T, Kudoh H, Sugimoto M, Hama Y Nucl. Inst. and Meth. B 151, 154 (1999)

[47] A. Kosemen, S. E. San, M. Okutan, Z. Dogruyol, A. Demir, Y. Yerli, B. Sengez, E. Basaran, F. Yılmaz, Microelectronic Engineering, 88, 17 (2011).

[48] A. L. Evelyn, D. Ila, R. L. Zimmerman, K. Bhat, D. B. Poker, D. K. Hensley, C. Klatt, S. Kalbitzer, N. Just, C. Drevet, Nucl. Instr. And Meth. In Phys. B 148, 1141 (1999).

[49] A. L. Stepanov, J Techn. Phys. 74, 1 (2004).

[50] J. D. Gi Winter H and Aumayr F., J. Phys. B: At. Mol. Opt. Phys. 32, 39 (1999).

[51] J. P. Briand, G. Giardino, G. Borsoni, V. Le Roux, N. Bechu, S. Dreuil, O, Tuske, G. Machicoane, Rev. Sci. Instrum.71, 627 (2000)

[52] Fischer B E and Metzger S., MRS Bull. 25, 39 (2000)

[53] A. Yamauchi, N. Yasuda, T. Asuka, T. Izumi, K.. Masutani, K. Oda, R. Barillon, Nucl. Instrum. Methods B 236, 318 (2005).

[54] S. Okuji, H. Boldyryeva, Y. Takeda, N. Kishimoto, Nucl. Instr. and Meth. in Phys. Res. B 242, 353 (2006) .

[55] W. Hong, H-J. Woo, H-W Choi, Y-S Kim, G-d. Kim, Appl. Surf. Sci, 169±170, 428 (2001)

[56] L. H. Sloof, A. van Blaaderen, A. Polman, G. A. Hebbink, S. I. Klink, F. C. J. M. van Veggel, J. W. Hofstraat, Appl. Phys. Lett. 91, 3955 (2002)

[57]J. Zhang, J. Kang, P. Hu, Q. Meng, Appl. Surf. Sci., 253, 5436 (2007).

[58] N. L. Singh, A. Qureshi, F. Singh, D. K. Avasthi , Mater. Sci. Eng., B 137, 85 (2007)

[59] M. Prasad, P. F. Conforti, B. J. Garrison, Y. G. Yingling, Appl. Surf. Sci. 253(15), 6382 (2007)

[60] P. F. Conforti, M. Prasad, B. J. Garrison, Appl. Surf. Sci. 253(15), 6386 (2007)

[61] P. F. Conforti, M. Prasad, B. J. Garrison, J. Phys. Chem., C 111(32), 12024 (2007).

[62] A. Licciardello, M. E. Fragal, G. Foti, G. Compagnini, O. Puglisi, Nucl. Instr. and Meth. B 116(1), 168 (1996)

[63] Y. T. Suetal., Nucl. Instr. and Meth. in Phys. Res. B 267, 2525 (2009)

[64] H. Kaczmarek, H. Chaberska, Appl. Surf. Sci. 252, 8185 (2006)

[65] M. Yedji, G. G. Ross , Nucl. Instrum. Methods Phys. Res., Sect., B 256, 396 (2006)

[66] R. K. Y. Fu, I. T. L. Cheung, Y. F. Mei, C. H. Shek, G. G. Siu, P. K. Chu, W. M. Yang, Y. X. Leng, Y. X. Huang, X. B. Tian, S. Q. Yang, Nucl. Instrum. Methods Phys. Res., Sect., B 237, 417 (2005)

[67] J. Micromech. Microeng. 18, 104015 (2008)

[68] Schenkel T, Hamza A V, Barnes A V, Schneider DH. Prog. Surf. Sci., 61, 23 (1999)

[69] F. I. Allen, A. C. Biedermann, R. Radtke, G. Fussmann, Review Of Scientific Instruments 77, 03b903 (2006)

[70] J.F. Ziegler, J.P. Biersack, M.D. Ziegler, SRIM - The Stopping and Range of Ions in Matter, SRIM Co., Chester, MD, 2008

[71] D.V. Sviridov, Russ. Chem. Rev. 71, 315 (2002)

[72] D Singh, Journal of Non Crystalline Solid, 256 (2010)

[73] S Yoshimura, K Ikuse, Y. Tsukazaki, M. Kiuchi, S. Hamaguchi, Journal of Physics: Conference Series 191, 012030 (2009).

[74] J. Robertson, E.P. O'Reilly, Phys. Rev. B 35, 2946 (1987).

[75] J. Davenas, P. Thevenard, G. Boiteux, M. Fallavier, X.L. Lu, Nucl. Instrum. Method B 46, 317 (1990).

[76] S. Kawato, T. Hattori, T. Takemori, H. Nakatsuka, Phys. Rev. B 58, 6180 (1998).

[77] J.P. Biersack, R. Kallweit, Nucl. Instrum. Methods B 46, 309 (1990).